STRUCTURAL STUDIES OF BOTULINUM NEUROTOXIN PROGENITOR
COMPLEXES AND TETANUS NEUROTOXIN

By

Desirée Allyn Benefield

Dissertation

Submitted to the Faculty of the

Graduate School of Vanderbilt University

in partial fulfillment of the requirements

for the degree of

DOCTOR OF PHILOSOPHY

in

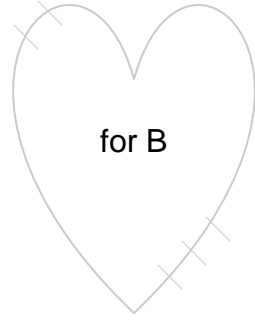Microbiology and Immunology

August, 2014

Nashville, TN

Professor D. Borden Lacy

Professor Earl Ruley

Professor Melanie Ohi

Professor Timothy Cover

Professor Eric Skaar

for B

ACKNOWLEDGEMENTS

I would like to sincerely thank Dr. Borden Lacy for the opportunity to do my thesis research in her laboratory. Borden has been a kind, patient, and encouraging mentor. She has taught me how to be a better scientist, to think more critically, and to use my artistic impulses as tools for addressing questions in my research. Thank you, Borden, for taking a chance and welcoming me into your lab. Thank you for suggesting structural projects that played to my strengths and for giving me the opportunity to explore areas of structural biology that excited me.

I would also like to thank my lab mates for keeping things interesting. It has been an adventure and I'm glad to have known and worked with you. I really appreciate the technical advice and laboratory guidance offered by Stacey Seeback, Heather Kroh, Rory Pruitt, Kelly Gangwer, and Darren Mushrush. My collaborations with Dr. Melanie Ohi's lab members have been equally fulfilling and educational. I am extremely fortunate to have had the opportunity to learn from and work with Yoshi Takizawa and Melissa Chambers. You are generous teachers.

Being from Nashville, I've always known about and respected the institution that is Vanderbilt University and being a part of this institution has been an honor for which I am deeply grateful. Entering through the Interdisciplinary Graduate Program gave me the opportunity to discover and learn about different fields of biomedical research and it also helped me find my way to the

TABLE OF CONTENTS

LIST OF TABLES

viii

LIST OF FIGURES

LIST OF ABBREVIATIONS

BoNT   botulinum neurotoxin

TeNT   tetanus neurotoxin

CNT   clostridial neurotoxin

NAP   neurotoxin associated protein

PC   progenitor complex

HA   hemagglutinin-like

NTNH   non-toxin, non-hemagglutinin

MLD_{50} mean lethal dose

SV   synaptic vesicle

LC   light chain, catalytic domain

SNARE   soluble N-ethymaleimide-sensitive factor attachment protein

                    receptor

SNAP-25   synaptosonal-associated protein of 25 kDa

PNS   peripheral nervous system

CNS   central nervous system

HC   heavy chain

RBD   receptor binding domain

TD   translocation domain

Syt   synaptotagmin

VAMP   vesicle-associated membrane protein

EM   electron microscopy

3D	three-dimensional
2D	two-dimensional
RCT	random-conical tilt
mrc	mixed rastor content
SDS-PAGE	sodium dodecyl sulfate polyacrylamide gel electrophoresis
FSC	Fourier shell correlation
HC_N	N-terminal translocation domain
HC_C	C-terminal binding domain
GABA	γ-aminobutyric acid
LB	luria broth
OD_{600}	optical density, absorbance at 600 nm
IPTG	Isopropyl β−D−1−thiogalactopyranoside
pdb	protein data bank
siRNA	small interfering RNA

Chapter 1

INTRODUCTION

The Clostridia species *Clostridium botulinum* and *Clostridium tetani* are known for their ability to produce and release two incredibly potent and deadly neurotoxins. These toxins, botulinum and tetanus, have a long history as neuroparalytic agents in man that continues into modern times. Considerable work has been done to define and understand the mechanisms of pathogenesis attributed to these toxins. These toxins are remarkable in their similarity and their differences in both form and function. Structural aspects of both toxins continue to be defined and examined. Here, I present structural analyses of tetanus neurotoxin and botulinum neurotoxin progenitor complexes. Results from this work improve our understanding of their structural organization and helps us to conceptualize the role of their structure during disease.

Historical Overview

Pathogenic microbes have sickened people since our earliest societies; our history is full of accounts of pandemics and plagues [1,2]. The origins of infectious diseases were ill defined and mysterious. By the 16th century there was limited recognition that a "contagion" was at work in some diseases, such as syphilis [3] or bubonic plague [4], yet the contagion itself remained unrecognized.

During the 17th century Robert Hooke and Antoni van Leeuwenhoek each manufactured their own microscopes and observed the microorganisms that inhabited an unseen world [5]. The correlation between microbes and disease was not recognized at the time. However, their introduction of the microscope and the discovery of microorganisms began mankind's foray into microbiology.

The research and findings of Louis Pasteur and Robert Koch during the mid to late 19th century marked the beginning of an era for the germ theory of disease. The work of the these two individuals not only exposed the vastness of the microbial world but also defined specific guidelines for the study of these organisms and their role in disease [6]. It was with these tools in hand that researchers began to define the causative agents of many microbial related diseases.

The neuroparalytic diseases botulism and tetanus have sickened humans and animals for thousands of years. The debilitating flaccid or spastic paralysis associated, respectively, with these two diseases is the result of intoxication with either botulinum neurotoxin (BoNT) or tetanus neurotoxin (TeNT). Each clostridial neurotoxin (CNT) is produced by bacteria commonly found in soil. The existence of these bacteria and their damaging neurotoxins wasn't discovered until the late 19th century [7,8]. The diseases associated with the toxins continue to be of serious medical concern but are also appreciated for their potential in beneficial clinical applications.

Historically, tetanus is most associated with military medicine. Its earliest accounts coincide with observations made on wounded soldiers. Symptoms of tetanus are described as spastic paralysis in a soldier with a head injury in a 3,500-year old Egyptian surgical treatise [9]. The term tetanus comes from the Greek word *tetanos*, a derivation of *teinein*, to stretch. In the 4th century Hippocrates described the symptoms of tetanus in his writings [10]. The painting *Opisthotonos* by Sir Charles Bell [11] depicts a wounded soldier from the Napoleonic Wars locked in a hyperextended spasm. The connection between wounds and the symptoms of tetanus were recognized in early medicine, but the details of their relationship would not be discovered until the late 19th century.

In contrast to tetanus, accounts of botulism before the 18th century are rare because the association of paralytic death and food consumption was not yet recognized. However, it has been theorized that ancient dietary laws and taboos may have originally been created to discourage the intake of poisonous food [12]. During the Middle Ages an edict from Emperor Leo VI of Byzantium forbade the consumption of blood sausages after what likely was a botulism outbreak [13] suggesting an awareness of the link between poisoned food and paralysis. When an outbreak of botulism occurred in 18th century Germany members of its medical community investigated the cause and linked the sickness to consumption of blood sausages. Theories on the "sausage poisoning" origin ranged from food contamination with cyanide to, notably, the presence of a *zoonotic or organic poison* [12]. An early 18th century medical

officer named Justinus Kerner became the first person to document cases of foodborne botulism. His systematic account of cases and their observed symptoms culminated in an 1820 monograph on sausage poisoning. Kerner suggested the disease was caused by "fatty acid", a biological poison, [14] that had developed in the sausage. In 1870 John Müller, a German physician, renamed the sickness related to "sausage poisoning" to "botulism" using the Latin word for sausage, *botulus* [15]. It would be another 30 years before the causative agent of botulism was identified as a bacterial toxin.

In 1884 Antonio Carle and Giorgio Rattone proved that tetanus was an infectious disease. They reproduced the disease in rabbits by inoculation with pus from a wound of a tetanus victim. They hypothesized that the spastic paralysis of tetanus was due to a causative agent living in nerves [16]. Also in this year, Arthur Nicolier observed the development of tetanus in animals after injecting them with soil. Upon looking at the soil samples by microscope he observed numerous rod-shaped bacteria present. The same bacteria were also recovered from the injection site on the rabbits, leading him to hypothesize that these bacteria were the source of the disease. He proposed naming the bacteria *Bacillus tetanus* [8]. He found no evidence that the bacteria spread throughout the body and instead suggested that a toxic substance was released from the bacteria at the site of infection [17]. Shibasburo Kitasato, a researcher trained in Robert Koch's laboratory, successfully isolated *Bacillus tetanus* from the wound of a patient in 1889. This was an impressive feat. Initially, his specimen

contained multiple species of bacteria including a population of spores. By heating the sample he killed the other bacteria and recovered a pure sample of the sporulated bacteria. He discovered that the bacteria would only grow in an anaerobic environment. Upon having a pure culture of *Bacillus tetanus* he satisfied Koch's postulates and confirmed that this isolated organism was the source of tetanus [7]. A year later in 1890 Knud Faber, a Dutch scientist, demonstrated that a soluble protein released by the bacteria in its growth medium was the actual source responsible for all of the symptoms of tetanus [18]. Also in this year, Emil Behringand and Kitasato published a report for a potential tetanus antitoxin [19]. They demonstrated that rabbits inoculated with non-lethal doses of pure *C. tetani* culture were no longer at risk when challenged later with a lethal concentration of the bacteria. They also injected whole blood or serum from the pre-treated rabbits into mice. The mice that had received blood or serum from the pre-treated rabbits survived subsequent challenge with the bacteria, thus indicating that something in the blood could inactivate the toxin. This important discovery not only introduced a real possibility for the prevention of tetanus and other toxin mediated diseases [20] but also introduced the world to the nascent field of immunology.

In 1895 Emile Pierre Marie van Ermengem, another microbiologist trained in Robert Koch's laboratory, determined the true source of botulism when several people became fatally ill with the disease after eating raw salted ham. Ermengem isolated rod-shaped, anaerobic bacteria from both the ham and the organs of a

victim and showed that this organism produced flaccid paralysis in test animals. In his 1897 report he proposed naming the new bacteria *Bacillus botulinus*. He also determined that a soluble protein released by the bacteria into its liquid culture was sufficient to cause botulism in test animals [8].

Based on the work of Kerner and Van Ermengem it was assumed that botulism only occurred in contaminated meat. This assumption changed in 1904 after a lethal outbreak of botulism was traced back to *Bacillus botulinus* in canned beans [21]. In 1910 antitoxins that were made for the bacteria isolated from salted ham in 1897 and the beans in 1904 were tested against one another. This test revealed that the two strains were immunologically distinct and therefore required different neutralizing antitoxins [22]. These BoNT serotypes were later classified alphabetically as type A and type B [23].

The revelation that BoNT possesses genotypic diversity has prompted over 100 subsequent years of research in pursuit of understanding its serological differences and the bacteria that produce them.

Neurotoxigenic Clostridia

Classification

To differentiate between *aerobic*, spore-forming organisms and *anaerobic,* spore-forming organisms the 1924 Committee on Classification of the Society of American Bacteriologists suggested use of the generic terms *Bacillus*

6

and *Clostridium* [24]. As a result, the neurotoxigenic, anaerobic bacilli were now classified as either *Clostridium tetani* or *Clostridium botulinum.*

The genus Clostridium contains over 100 species, 35 of which are pathogenic [25]. The genus varies phylogenetically but is traditionally defined as: gram positive, spore-forming, anaerobic, rod-shaped bacteria [25]. In unfavorable growth conditions, these bacteria produce an intracellular endospore to contain their genome and essential metabolic machinery before entering a dormant phase [26]. The endospores possess a thick protective coat that is resistant to a range of high temperatures and other environmental insults. The endospores of *C. tetani* and *C. botulinum* are wider than the cell and located at its terminal end [27] giving the bacteria a 'spindle-like' shape from which the name *Clostridium* derives [13].

The neurotoxigenic clostridia *C. tetani* and *C. botulinum* are classified by which type of toxin is produced by the organism. This is a satisfactory approach for *C. tetani* because toxin synthesis only occurs in a uniform group of bacteria in this species and only one serotype of that toxin has been identified. The TeNT encoding gene is located on a plasmid and its presence or absence determines whether or not the organism is toxigenic [13,28].

Classification of *C. botulinum* is more complicated due to the phylogenetic diversity of the organisms that can produce BoNT. For this reason *C. botulinum* is reserved for *all* bacteria with the ability to produce the neurotoxin [29]. From the early 1900s to as recently as 2013 eight different immunologically distinct

serotypes (designated with the letters A-H) have been identified [29,30]. Multiple subtypes within each serotype have been determined by differences in amino acid sequence [29,30]. The taxonomy of the organisms that produce BoNT includes members of *C. botulinum, C. argentinense, C. butyricum*, and *C. baratii* all of which have been classified into six groups representing their physiological and genetic differences [31,32] (Table 1-1).

Group I contains proteolytic *C. botulinum* serotypes A, B, F, and H. Bacteria in this group can release a variety of extracellular enzymes to obtain nutrients [33,34]. This group also contains an array of subtype strains some of which possess more than one neurotoxin gene that may or may not have activity [35]. Depending on the subtype, the BoNT gene is located either on the chromosome or a plasmid. BoNT/A and /B serotypes are commonly associated with food borne or wound botulism in humans [36]. Bacteria in this group form hardy spores that are distributed widely in soil.

Group II members are non-proteolytic bacteria and do not release extracellular enzymes. This group contains *C. botulinum* strains that produce BoNT serotypes and subtypes of B, E, and F [37]. Group II serotypes B and E are often associated with foodborne botulism from salted or smoked fish or meat [36]. Bacteria in this group only have a single neurotoxin gene that is located on either the chromosome or a plasmid [38]. Bacterial spores from this group are less heat resistant than Group I but remain widely distributed in soil and sediment [25].

C. botulinum serotypes and subtypes C and D are in Group III. These serotypes are heavily associated with avian and animal botulism. Strains in this group are either weakly proteolytic or lack proteolytic activity and the neurotoxin gene is located on a bacteriophage [29,39]. Groups IV – VI represent other clostridia species capable of producing BoNT [29,40]. *C. argentinense*, of Group IV, produces BoNT/G only. This proteolytic bacteria was originally isolated from Argentinian soil samples [41] and is not associated with botulism in humans. Groups V and VI contain neurotoxigenic strains of BoNT/E producing *C. butyricum* and some strains of BoNT/F making *C. baratii*. Both groups have been implicated in cases of human botulism [42,43].

Table 1-1. Characteristics of neurotoxigenic clostridia

Characteristic	C. tetani	C. botulinum			Group IV[1]	Group V[2]	Group VI[3]
		Group I	Group II	Group III			
Toxin Type	TeNT	A, B, F, H	B, E, F	C, D	G	E	F
Gene Location[4]	P	C, P	C, P	bp	P	C	P
Spore Heat Resistance[5]	84	104-121	77-82	104	82-120	30-37	30-37
Proteolysis	-	+	-	-	+	-	-

[1] *C. argentinense*
[2] *C. butyricum*
[3] *C. baratii*
[4] P = plasmid, C = chromosome, bp =bacteriophage [31,44,45]
[5] Heat resistance temperatures in °C

Toxin Genetics

TeNT is not associated with foodborne illness and BoNT is. Both neurotoxins are 150 kDa proteins that are susceptible to protease activity in the digestive tract. However, many *C. botulinum* strains produce BoNT and neurotoxin-associated proteins (NAPs). At low pH the toxin and NAPs non-covalently interact to form progenitor complexes (PCs) [30]. The NAPs include three hemagglutinin-like (HA) proteins (HA1, HA2, and HA3) and a non-toxin, non-hemagglutinn protein (NTNH). Other BoNT strains don't have the HA genes and produce smaller PCs. BoNT is orally toxic because the PC assembly protects the neurotoxin from degradation as it passes through the digestive tract [46,47]. TeNT has no NAP genes and forms no PCs making it susceptible to proteolysis [28]. These differences between the neurotoxins are reflected in their respective genetic organization. Figure 1-1 depicts the gene loci for TeNT and for the BoNT serotypes most commonly associated with foodborne botulism.

The TeNT gene locus consists of a single operon that contains genes for a neurotoxin expression regulator, *tetR*, *and* the neurotoxin. No genes for NAPs are present [48]. By comparison, the BoNT gene locus is comprised of two operons separated by *botR*, a *tetR* homologue that regulates BoNT and NAP expression [31,38,49,50]. Some serotypes and subtypes may vary in their 5' genetic organization, but the 3' part of the locus is conserved [38]. The HA genes are clustered together in one operon while the NTNH and BoNT are clustered in the other. The organization for type is E differs from A and B in that it does not

11

express HA genes or encode for the expression regulator botR. Rather than an

HA operon, the type E equivalent contains *orfX* genes. The function of the OrfX

proteins is currently unknown. The NTNH and BoNT/E genes are in a separate

operon adjacent to a p47 gene. The function of p47 has not been determined

either [51].
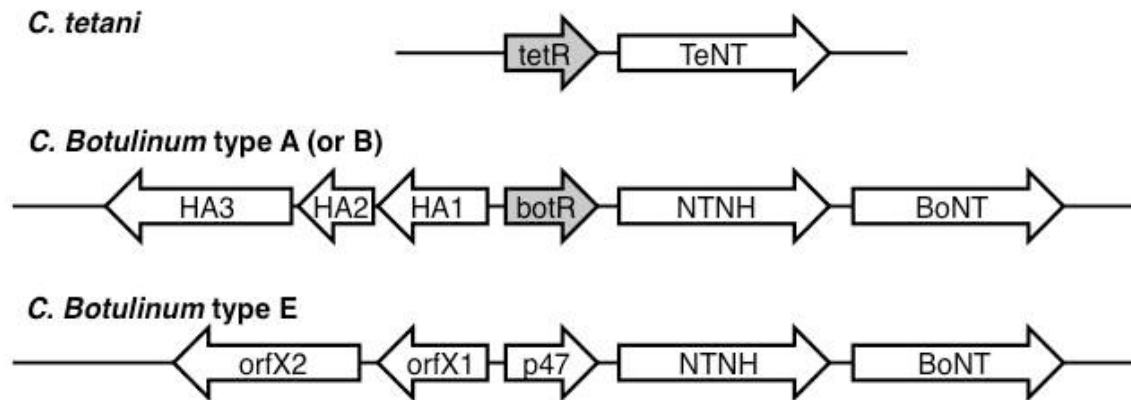
Figure 1-1. The genetic organization of TeNT and BoNT serotypes A, B, and E. *TeNT* in *C. tetani* is located in a single operon that contains an alternative sigma factor, *tetR*. The BoNT gene locus for toxins type A, B, and E in *C. botulinum* has two operons. One operon contains the HA genes and the other has the genes for *NTNH* and *BoNT*. The operons are separated by the alternative sigma factor, *botR*. *C. botulinum* type E does not express HA proteins and instead has an *orfX* operon adjacent to its *NTNH* and *BoNT* genes.

Virulence Factors and Toxicity

In addition to TeNT, *C. tetani* produces a second toxin named tetanolysin.

The gene for this second toxin is encoded for on the chromosome and is not

considered part of the TeNT gene locus [28]. This cholesterol-dependent

cytolysin can form pores and lyse red blood cells but its exact role in

pathogenesis continues to be defined. It is thought that this lytic activity may also

help TeNT disseminate through tissues [52,53]. The proteolytic *C. botulinum*

genome contains a nine-gene cluster that is highly similar to streptolysin from *Streptococus* [34] however there is no direct evidence that this results in a cytolytic toxin of its own. *C. botulinum* does, however, produce a binary toxin referred to as C_2 [54]. The toxin does not cause paralysis and is not considered a neurotoxin. The ADP-ribosylation activity of C_2 toxin interferes with actin assembly in the cell and alters cell function [55].

Recent genomic sequencing of *C. tetani* and representative Group I (proteolytic) *C. botulinum* strains has revealed that in addition to their neurotoxins and respective secondary toxins, there are several genes present whose products are predicted to influence the virulence of the organisms These include collagenases, fibronectin-binding proteins, surface layer proteins with adhesive properties, and chitinases [34,48]. Additional virulence factors for non-proteolytic *C. botulinum* are currently not well understood [37].

BoNT and TeNT are the principal virulence factors for their respective neurotoxigenic clostridia and are generally considered the first and second most potent toxic substances of biological origin [27]. The toxins share several characteristics, such as similar molecular weights, molecular structures, and modes of action. The potency of TeNT and BoNT has been evaluated in a number of animal models (reviewed in [56]) however toxicity estimates can be difficult to compare due to variations in assay and toxin purification [57,58]. Extrapolation from animal studies and accidental intoxication in humans suggests

that the calculated intravenous lethal doses for BoNT/A or TeNT are approximately 1 ng/kg and <2.5 ng/kg respectively [56,57].

Toxin produced by *C. botulinum* in culture or in foodstuffs exists as a heterogeneous population of free BoNTs, NAPs, and various sized PCs. Studies have shown that ingestion of free BoNT can be orally toxic if the dose is very high [59–61]. Interestingly, ingestion of BoNT in its complexed (PC) form dramatically increases its oral toxicity. The oral mean lethal dose (MLD$_{50}$) of the BoNT-PC in mice decreases as the PC size increases, suggesting that the larger PC assemblies promote BoNT passage through the gastrointestinal tract [62,63] (Table 1-2).

The BoNT and NAPs interact to form high molecular weight PCs. Ultracentrifugation studies on the complex have shown that the PCs regularly adopt three different sizes. These differences in size are indicated by their individual sedimentation rates. Uncomplexed BoNT has a molecular weight of 150 kDa and sedimentation rate of 7S. The other sizes formed include: 12S (M-PC, ~300 kDa), 16S (L-PC, ~500 kDa), and 19S (LL-PC, ~900 kDa). The 19S PC has only been observed with BoNT/A and is predicted to be a dimer of 16S PCs (reviewed in [30]). The PC sizes are dependent on the toxin serotype and the number of NAPs assembled in the complex.

Biochemical studies have determined that the NTNH protein association with BoNT is sufficient to protect the toxin form digestive conditions such as low pH in the stomach or the presence of digestive enzymes [47,64]. A recent

structure of a 12S complex shows the BoNT and NTNH as an interlocked complex that prevents degradation in acidic or proteolytic conditions [47]. The role of the HA proteins in the complex are less clear and theories continue to evolve. These will be discussed in more detail in the upcoming section on Research Objectives.

Table 1-2. BoNT PC size, NAP composition, and oral toxicities for serotypes commonly associated with disease in humans

Type	Molecular Size	Components	Oral LD$_{50}$[1]
A	19S, LL, 900 kDa	BoNT, NTNH, HA1, HA2, HA3 (a 16S dimer?)	120
	16S, L, 500 kDa	BoNT, NTNH, HA1, HA2, HA3	2,200
	12S, M, 300 kDa	BoNT, NTNH	3,600
	7S, S, 150 kDa	BoNT	43,000
B	16S, L, 500 kDa	BoNT, NTNH, HA1, HA2, HA3	1.5
	12S, M, 300 kDa	BoNT, NTNH	1,100
	7S, S, 150 kDa	BoNT	24,000
E	12S, M, 300 kDa	BoNT, NTNH	220
	7S, S, 150 kDa	BoNT	>750

[1]Oral LD$_{50}$ as equivalent number of i.p. LD$_{50}$ x 10^{-3}; in mice [62,63]

Tetanus and Botulism

Tetanus and Botulism are forms of infectious disease yet neither disease is contagious. The neurological dysfunction associated with each disease results from intoxication with either TeNT or BoNT. Both diseases manifest as forms of debilitating paralysis that are potentially life-threatening.

Symptoms

Generalized tetanus may occur in adults, infants, and animals after *C. tetani* spores are introduced to anaerobic conditions in a wound. This is the most common form of tetanus and represents the majority of documented cases. Neonatal tetanus is included in this category as it involves *C. tetani* infection in the umbilical cord stump [65]. The bacterial spores germinate in low oxygen conditions releasing TeNT into the body. The toxin binds to nerve terminals throughout the body to gain eventual entry into its target: motor neurons in the central nervous system (CNS). Symptoms occur when the neurotoxin prevents the release of inhibitory neurotransmitters at synaptic junctions used to quench nerve impulses. Symptoms of tetanus first appear in the head and neck region because of their shorter axonal pathways. The toxin prevents relaxation of inhibitory antagonist muscle groups and results in agonist and antagonist muscle groups contracting simultaneously [66]. Tetanus is commonly referred to as "lockjaw" because one of its first symptoms involves the tightening of jaw muscles until the infected individual can no longer open their mouth. Ironically, contractions in other facial muscles cause the appearance of a pained smile (25). An infected individual will experience painful, uncontrollable muscle contractions and spasms that descend into the chest and limbs. The spastic paralysis resembles convulsions and can be powerful enough to rupture tendons and fracture bones. The paralysis can also prevent normal respiration and can result in death if untreated [65]. Less common forms of the disease either only affect a

16

localized area around the wound (local tetanus) or only cranial nerves in the face after a head injury (cephalic tetanus) [67].

Botulism may also occur in adults, infants, and animals. Like tetanus, botulism can result from an infected wound but it also has four other recognized forms. Symptoms of botulism are the same regardless of its form and begin after exposure to BoNT. The neurotoxin disrupts signals at junctions between nerves and muscles in the peripheral nervous system and prevents muscle contraction [29]. Symptoms begin with fatigue, weakness and vertigo, usually followed by blurred vision, difficulty swallowing and talking. Facial muscle control is lost from palsy of the cranial nerves. The disease descends as a symmetric flaccid paralysis into the core and limbs. Nausea, constipation and abdominal swelling may also occur. In severe cases paralysis inhibits the contraction of respiratory and cardiac muscles and can result in death without treatment [68,69].

Botulism Forms

Wound

Much like tetanus, wound botulism occurs when a wound is contaminated with *C. botulinum* spores from the environment. The spores germinate in the anaerobic conditions of an abscess and BoNT is released into the body. This form of botulism was considered rare until recently. The condition has become more common since the early 1990s. The number of cases of wound botulinum has increased significantly worldwide and nearly all of these cases involve

17

heroin-injecting drug users [68]. The form of heroin being injected (either intravenously or subcutaneously) is a dark colored morphine derivative that is considered less refined than white heroin. Called black tar heroin, it is 'cut' or diluted with a variety of substances including soil. As a result *C. botulinum* spores can inadvertently contaminate the drug and be exposed to wounded areas on a drug-user [70].

Foodborne

The foodborne version of botulism is considered the classical form of the disease because of its history with food [69]. While tetanus is only associated with compromised wounds, botulism can also occur as a result of ingesting preformed-BoNT PCs in contaminated food. *C. botulinum* spores can survive many food preservation methods designed to kill nonsporulating organisms [71]. The spores can vary in their resistance to heat and many strains require temperatures above boiling to ensure their destruction. Surviving spores germinate and release toxin complexes in foods with an anaerobic environment, a pH over 4.5, and low sugar or salt content [72]. Foodborne botulism primarily occurs because the naturally occurring complexed form of BoNT is protected as it passes through the gastrointestinal tract [46,47]. Once in the small intestine the toxin makes its way into the bloodstream and then selectively targets and binds to neurons in the periphery [73]. BoNT serotypes /A, /B, and /E have each been associated with foodborne botulism.

Intestinal (Adult and Infant)

In contrast to foodborne botulism, intestinal botulism results from absorption of BoNT produced *in situ* by ingested *C. botulinum* spores that have germinated and colonized the gastrointestinal tract. Adult cases are rare and generally involve individuals who have had surgical procedures on their bowels and are on antibiotics [74,75]. Antibiotics in adults can reduce the population of normal flora in the intestine providing *C. botulinum* an anaerobic environment with limited competition from other species of bacteria.

Infant botulism is the most common form of the disease and also occurs when *C. botulinum* colonize the intestine and produce BoNT *in situ* [68]. Infants under the age of one are susceptible because their intestinal flora are not established enough to compete with *C. botulinum.* This disease is most associated with infants consuming honey (which can contain *C. botulinum* spores) but cases have also been linked to improperly home-canned baby food and contaminated milk products [76]. Botulism symptoms in infants resemble the adult form of flaccid paralysis but also include constipation, weak cry, inability to feed, loss of head control, and decrease in spontaneous movements [36,37].

Inhalation

This form of botulism is not a naturally occurring disease but its extreme potency and the increasing risk of bioterrorism requires that its threat potential be considered. The disease could potentially be acquired from the absorption of

deliberately released aerosol of the toxin. Studies have shown that inhaled BoNT/A can bind and transcytose across airway epithelial cells and eventually cause disease [77].

Iatrogenic

This is a recent form of botulism that can be caused by injection of BoNT for cosmetic or therapeutic purposes. Recommended doses for cosmetic uses are too low to cause disease symptoms however there have been observed botulism-like symptoms after intramuscular injections of the toxin [78]. Four people became extremely sick after receiving injections of unlicensed, highly concentrated BoNT for cosmetic purposes in 2004 [79].

Epidemiology

C. tetani and *C. botulinum* spores can endure many adverse conditions and as a result these bacteria are widely distributed in nature. Intoxication with either toxin is generally regarded as a "rural" concern but the toxigenic spores are ubiquitous and can cause disease in urban and non-urban communities [80–83]. Spores of toxin producing strains can germinate in practically any anaerobic environment with adequate energy sources [29].

Tetanus transmission occurs when wounds become contaminated with *C. tetani* spores. Tetanus is a vaccine preventable disease and cases are relatively rare in many developed nations due to wide spread vaccination efforts. However,

cases persist in the un-vaccinated or with intravenous drug users [67]. The disease remains prevalent (especially neonatal tetanus) in the developing world where disease treatment is usually inaccessible or unaffordable [84].

Cases of infant or wound botulism have continued to increase in frequency worldwide while cases of foodborne botulism remain comparatively rare [85]. Most foodborne outbreaks are limited in their size and the disease is normally traced back to the consumption of improperly prepared home-canned foods. Pickled, salted, or smoked fish dishes have also been implicated in outbreaks [68]. Industrial food processing techniques employ a number of preventative measures to reduce the potential for *C. botulinum* spores in food products; the disease severity and the threat of widespread exposure to poisoned food require them. However, commercial food products are still vulnerable, and companies understand the public relations and financial risks foodborne outbreaks can provoke [86–89].

Treatment

In 1890, Behring and Kitasato [19] discovered the presence of tetanus antitoxin in the serum of animals who survived lethal challenges with the toxin. The tetanus antitoxin was specific to TeNT and could not protect against a challenge with another type of toxin. The potential for passive immunization treatments in humans became immediately apparent. Sheep and horses were used to scale up production of antitoxins against diphtheria [90] or TeNT. To

21

prevent allergic reactions against the antitoxin containing animal serum, a tetanus vaccine was pursued. A 1924 publication from the Pasteur Institute detailed the procedure for making an effective tetanus toxoid vaccine using toxin exposed to formaldehyde and heat [91]. By 1926 the tetanus toxoid was used as a vaccine in humans [92] and it is essentially the same formulation used today. Further advances for tetanus vaccination involve the addition of adjuvants to stimulate a stronger immune response [93].

Work on the tetanus vaccine laid the groundwork for the development of the first botulinum vaccine in 1924 [94] and the first reported use of botulinum toxoid on humans came in 1934 [95]. A bivalent type AB toxoid was developed for use by soldiers during World War II [96]. Currently, there are two primary antitoxins available for the treatment of botulism. These antitoxins are collected from horse serum and are formulated to neutralize multiple serotypes, however, these toxoids are not widely available and are generally reserved for military personnel and laboratory researchers at risk of exposure [97]. Infant botulism is treated with an antitoxin derived from human serum rather than horse to prevent possible allergic reactions [98,99].

Both TeNT and BoNT can be prevented by vaccination. The only specific treatment for tetanus or botulism entails the administration of the appropriate antitoxin. The antitoxin can only neutralize toxin molecules that have not yet bound to nerve endings. Toxin neutralization reduces disease severity but paralytic symptoms cannot be stopped once the toxins have entered their target

neurons. Additional treatment strategies may include treatment with antibiotics to eradicate toxin-producing clostridia in wounds. Patients with tetanus may be sedated to reduce the severity of spasms [66] and severe cases of either disease require mechanical ventilation and supportive intensive care treatment to prevent death from acute respiratory failure. Cases of tetanus may necessitate intensive care unit admission for 3-5 weeks [66] while cases of botulism may require weeks to months of hospital care [68].

Neurotoxins as Bioweapons and Medicine

Humans have used bioweapons throughout history. Disease-causing agents such as viruses, bacteria, or toxins have been utilized for assassinations or against entire populations [100]. Bioweapons wield great power in their *potential* to cause massive casualties to an enemy, however their actual efficacy largely depends on factors such as potency, stability, delivery and dispersal [101]. Regardless, bioweapons also possess a *psychological* power. They have the power to reduce a population to panic and overreaction [102].

There have been numerous attempts to use BoNT as a bioweapon. The relative ease of its cultivation and its extreme potency make it an attractive candidate for use. The threat of a bioterrorist attack with BoNT is considered a credible risk and many measures have been imposed to regulate the toxin and to prepare health workers in the wake of a large outbreak [103–106]. At the Centers for Disease Control, potential biological terrorism agents with the ability to inflict

23

mass casualties, public fear, and civil disruption are classified as category A select agents. Members of this group include anthrax, small pox, plague, and botulinum neurotoxin.

Paradoxically, in recent years BoNT has been recognized for its therapeutic potential in the treatment of a number of disorders characterized by involuntary movements from hyperactive muscles [107]. BoNT is able to disrupt neurotransmission required for muscle contraction, often for prolonged periods, and clinicians now use small, localized doses of the toxin to alleviate the symptoms of several muscle disorders including: head, neck, and limb dystonias, hemifacial spasms, blepharospasm, and hyperhidrosis (reviewed in [108]). TeNTs disruption of neurotransmitters required for muscle relaxation has not yet been used as a therapeutic [28]. However, there is growing interest in exploring TeNTs biological properties as a means of addressing other neuromuscular disorders.

Role of the Neurotoxins in Disease

Molecular Targets of TeNT and BoNT

Once in the bloodstream, TeNT and *un*complexed BoNT target receptors located on the plasma membrane of peripheral nerve endings [65]. Gangliosides are found in abundance on the surface of neuronal cells [109,110] and studies *in vitro* and *in vivo* have shown that they act as receptors for the CNTs [111−116].

BoNTs also use proteins from the lumen of synaptic vesicles (SV) as co-receptors [117–121] which has led to a dual-receptor hypothesis. It has been suggested that gangliosides either direct CNTs to areas of the neuronal membrane that are enriched in protein receptors or keep the toxins in a conformation favorable to receptor binding [122,123]. It is unclear if TeNT requires a protein co-receptor or instead relies on interaction with two distinct gangliosides [124,125]. Regardless, CNT binding to receptors on the surface of motor neurons triggers a clathrin dependent internalization event [126–128].

The differences between the clinical symptoms of tetanus and botulism are the result of differences in toxin transport once in the cell (Fig. 1-2). The long held model for CNT neuronal uptake and trafficking holds that BoNTs exploit SV endocytosis and recycling for entry into motor neurons. As a result BoNT remains localized at neuromuscular junctions in the peripheral nervous system (PNS). SVs lower their pH in order to reload with neurotransmitters and this acidification leads to the BoNT translocation domain inserting into the SV membrane and the release of its catalytic domain, the LC, into the neuronal cell cytosol [129,130]. By contrast, after TeNT entry into the motor neuron the toxin is sorted into the fast axonal retrograde transport endosome that goes to the motor neuron soma in the spinal cord [131,132]. These endosomes do not acidify [129,133] which prevents translocation domain membrane insertion and LC release into the cytoplasm thus allowing TeNT to remain intact for the remainder of its transport [116]. TeNT crosses the intersynaptic space between the motor neurons and the inhibitory

neurons of the spinal cord where it is internalized by a SV. This vesicle does acidify and will release the TeNT LC into the cytosol.

The BoNT and TeNT LCs are metalloproteases that selectively target and cleave specific SNARE proteins (soluble N-ethylmaleimide-sensitive factor attachment protein receptors) that mediate the assembly of the SV docking-fusion complex. Proteins that are part of this assembly include: synaptobrevin, syntaxin, and SNAP-25 (synaptosomal-associated protein 25) [134]. TeNT, BoNT/B, /D, and /F cleave at different scissile bonds on synaptobreven, BoNT/A and /E cleave SNAP-25 and BoNT/C can cleave either SNAP-25 or synatxin. Cleavage on any one of these proteins disrupts the complex assembly and SVs can no longer release their neurotransmitter cargo. BoNT disruption of the SNARE complex prevents the release of acetylcholine neurotransmitters at the neuromuscular junction that results in flaccid muscle paralysis and dysfunction in the autonomous nervous system associated with botulism [135,136]. TeNT disruption of the SNARE complex inhibits the release of inhibitory neurotransmitters required for muscle relaxation and results in the spastic paralysis attributed to tetanus [129,137,138].

Over the past 50 years there have been intermittent reports of BoNT affecting the CNS [139,140] though how it did this remained unclear. Several recent experiments have explored this possibility further and have sought to better understand the mechanisms that effect the intracellular sorting and fate of CNTs in the PNS and CNS. For example, it was recently demonstrated that
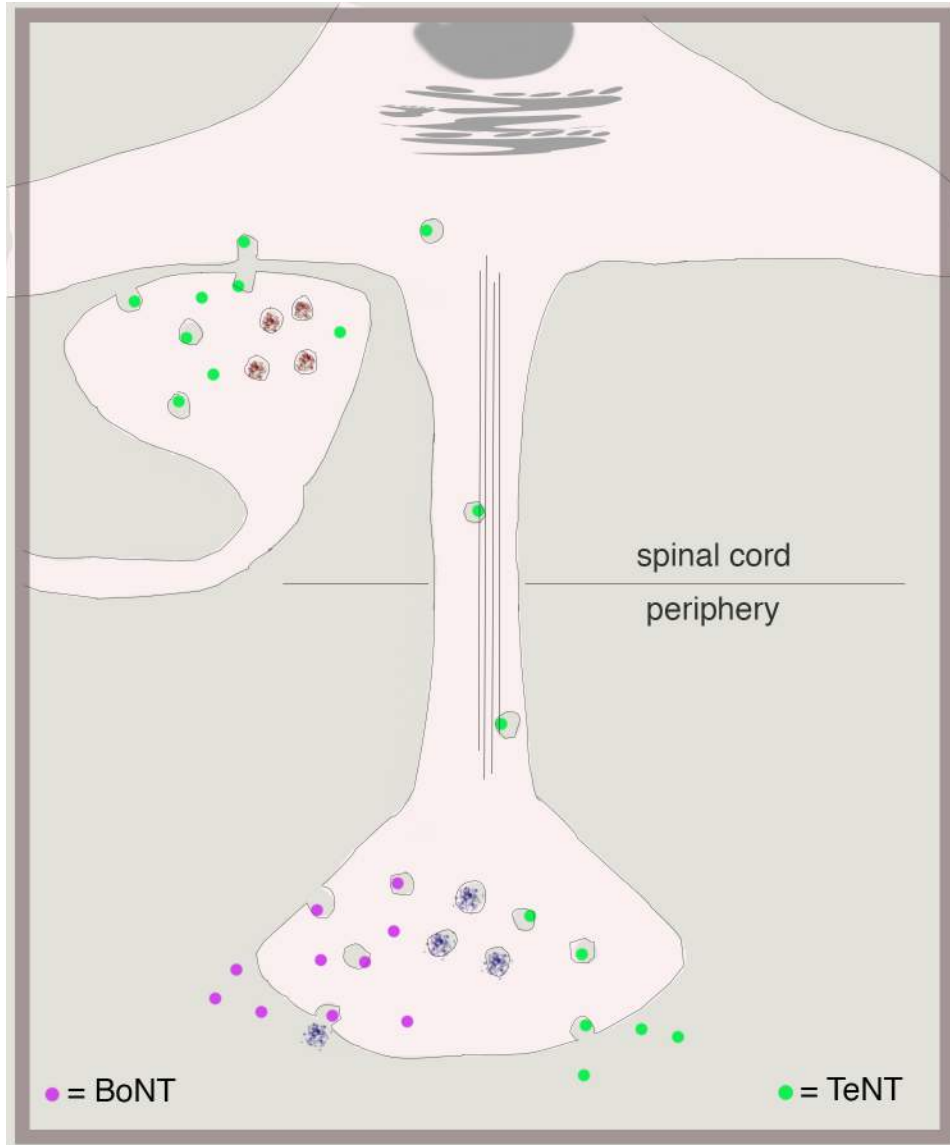
Figure 1-2. A schematic view of a motor neuron interacting with a spinal cord inhibitory interneuron. The sites of action for BoNTs (purple dots) at the neuromuscular junction where synaptic vesicles can no longer release their neurotransmitter cargo (small, blue dots) and TeNTs (green dots) undergoing axonal retrograde transport. TeNT crosses into the inhibitory interneuron and prevents neurotransmitter release (small, red dots).

BoNT serotypes /A and /E are capable of retrograde transport in primary spinal

cord neurons [141,142]. Many mechanistic questions remain regarding how the

CNTs are sorted and transported in neurons, but it is already clear that the paradigm model of CNT trafficking in neurons is incomplete.

TeNT and BoNT Structure and Function

Both TeNT and BoNT are produced as inactive ~150 kDa single-chain proteins. The chains are post-translationally nicked into active dichain molecules [143] that consist of a 50 kDa light chain (LC) and a 100 kDa heavy chain (HC) linked by an interchain disulfide bond. CNTs have an AB toxin organization and consist of three ~50 kDa functional domains: binding (RBD), translocation (TD), and catalytic (LC) (Fig. 1-3a). The binding domain spans the C-terminus of the HC while the translocation domain makes up the N-terminal half of the HC. The catalytic domain, found at the N-terminus of the protein, is the LC and functions as a zinc-endopeptidase specific for core components of the neurotransmitter release apparatus [144,145]. The structures for BoNT/A, /B, and /E holotoxins have been determined [146–148]. Types /A and /B share a similar structural organization while type /E has a unique organization (Fig. 1-3b). The structure of the TeNT holotoxin is unknown but two of its three domains have high-resolution structures available and have similar structures to their BoNT homologues (Fig. 1-3c and 1-3d) [145,149]. The three CNT domains each have their own function but recent work by Fischer *et al.* [150] suggests that they also work in concert so that each domain chaperones the other through the intoxication process.
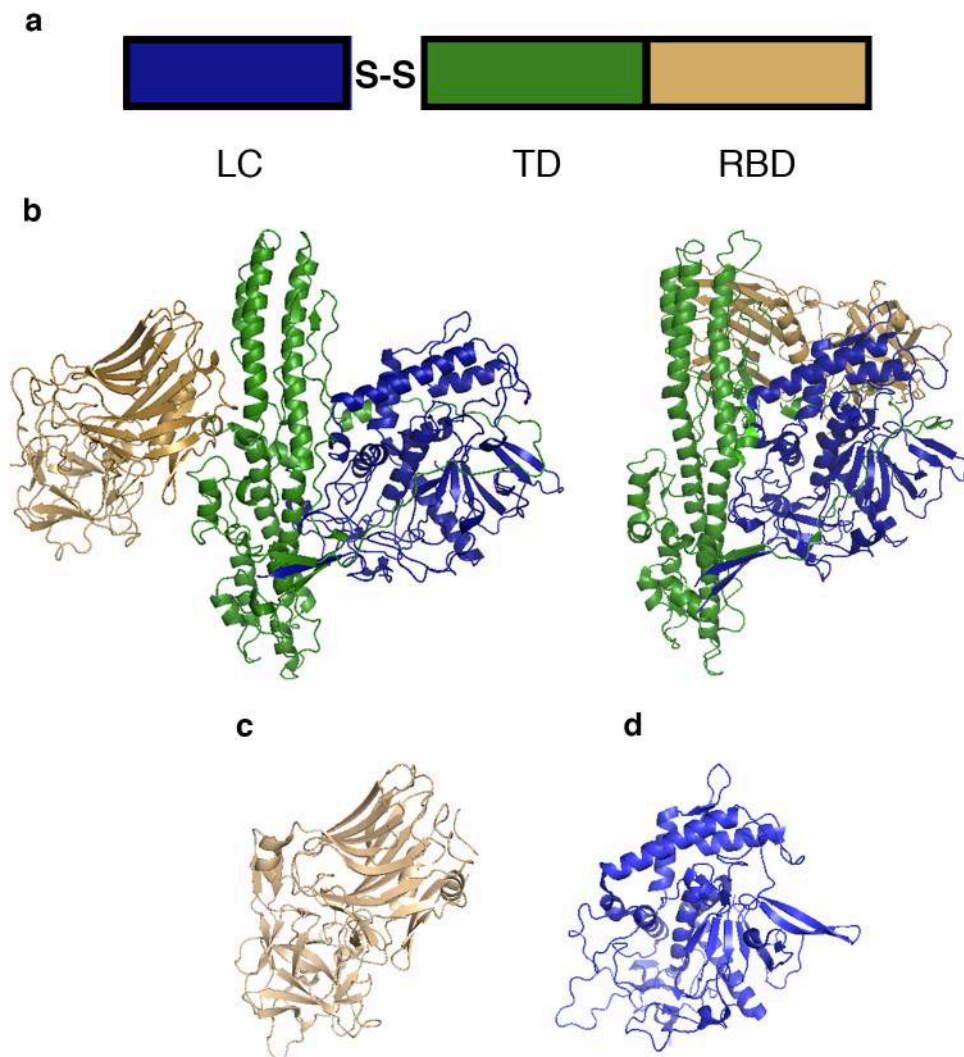
Figure 1-3. The structural organization of the CNTs. (a) The activated CNT has three domains linked by a disulfide bridge: the catalytic domain (LC in blue), the translocation domain (TD in green), and the receptor-binding domain (RBD in beige). (b) The structures of BoNT/A (left) and BoNT/E (right) have different organizations [146,148]. (c) The TeNT RBD [149] and (d) LC [145]. The TeNT holotoxin structural organization is unknown.

Receptor Binding

     C. tetani in wounds can produce and release TeNT and other virulence factors such as tetanolysin. The lytic activity of tetanolysin may assist TeNT in gaining entry into the bloodstream where it can then target the plasma membrane of peripheral nerve terminals. The TeNT receptor binding domain (RBD) structure has been determined [112,149,151,152] and is structurally similar to the BoNT/A RBD. The RBD is comprised of two subdomains, an N-terminal beta-barrel and a C-terminal beta-trefoil fold [153]. For TeNT, these subdomains can simultaneously bind two polysialogangliosides found on the surface of the neuronal cell [28,125] to induce endocytosis.

     When considering receptor binding for BoNT one must take into account how the toxin reaches the bloodstream. If the toxin is released as a result of wound botulism its process is much like that of TeNT. BoNTs use two independent receptors to gain access into the neuronal cell. BoNTs first interact with gangliosides on the cell surface and then interact with specific protein receptors. The three serotypes that cause human botulism, types /A, /B, and /E, have been found to bind to the same subset of gangliosides (reviewed in [114]) and their protein receptors are also known. The protein receptors for BoNT/A and /E have been identified as synaptic vesicle protein 2 (SV2) while BoNT/B binds to synaptotagmin I or II (Syt I or Syt II) proteins [117,119,154,155]. The overall structure of TeNTs RBD is very similar to the BoNT RBD. The two toxins share

significant sequence homology in the N-terminal binding subdomain as compared to their C-terminal subdomains [156].

Translocation

The translocation of the CNT LC into the neuronal cell cytosol is essential for pathogenesis to occur. Study of the actions of this domain has refined our understanding on the elegant design of the neurotoxin and how all three of its domains guide one another during the translocation process [150,157–159]. There has been extensive work done to understand the structure and function of these toxins. Currently, there is more literature available for BoNT than TeNT on the translocation event, but due to their structural and functional homology it is likely that the process is similar between the toxins.

After the CNT has entered a neuron it must be able to translocate its catalytic domain into the cytosol. The synaptic vesicles that BoNT and TeNT use to gain entry into neurons (at the neuromuscular junction or at inhibitory interneurons in the spinal cord) produce a pH gradient in the lumen using a vesicular ATPase proton pump [160]. The acidification of these SVs induces a conformational change in the toxin structure allowing its translocation domain to form a pore in the vesicle membrane so that the LC is released into the neuronal cell cytosol. Recent experiments have shown that this conformational change and membrane insertion are dependent on RBD interaction with polygangliosides in the SV lumen [160,161] and that specific residues in all three domains of the

toxin are responsible for pH sensitivity [162]. It has been demonstrated that the TD protects the LC while in the acidic lumen environment and will eventually guide its exit from the SV [163]. CNTs with broken interchain disulfide bonds cannot form channels [164] and the LC will not be translocated. The LC is partly unfolded to exit the SV. Once out of the lumen the disulfide bond is reduced and the LC is free in the cytosol [157].

Catalytic

The LC is probably the most studied domain in CNTs and has prompted numerous structural and biochemical investigations. Crystal structures are available for BoNT serotypes /A - /G as well as for TeNT (reviewed in [165]). All CNT LCs share a similar globular fold, and they all share a characteristic zinc-binding motif (HExxH+H) for their active sites. The zinc is bound inside a large cavity with a high negative electrostatic potential. The LCs all use the same catalytic mechanism but interestingly the BoNT serotypes target different substrates of the neurocytosis apparatus with high specificity. This specificity is attributed to interactions with the substrate that are independent of the active site [166]. Each LC will target and cleave a specific scissile bond related to specific SNARE proteins that mediate SV docking and fusion [166,167]. TeNT and BoNT/B, /D, and /F recognize and cleave different scissile bonds located on a vesicle-associated membrane protein (referred to as VAMP or synaptobrevin). BoNT/A and /E specifically recognize and cut different peptide bonds on SNAP-

25 while BoNT/C will cleave both syntaxin and SNAP-25 (reviewed in [168]). In addition to their holotoxin structures, some LCs have been co-crystallized with their targeted SNARE substrate [121,155,169] allowing for additional insight in understanding the specificity of each toxin.

Research Objectives

In the case of foodborne botulism the toxin must cross through epithelial cells in the intestine to gain access to the bloodstream. It is important to remember that in addition to BoNT, *C. botulinum* also releases NAPs that non-covalently associate with the toxin to form a heterogeneous population of toxin complexes. The complexes are pH-sensitive, and disassemble at pH ≥ 7 [170–172]. BoNT and NAPs produced at the site of an infected wound likely will not assemble into a PC because the pH of the circulation system is slightly basic [173]. Ingestion of BoNT PCs from contaminated food is orally toxic because the toxin is protected from the low pH of the stomach and the presence of digestive enzymes. Once the stomach content empties into the duodenum pancreatic bile salts are released to neutralize the low pH of the chyme from the stomach [174]. The duodenum pH is maintained between 6 and 7 [175]. The question of whether the NAPs remain associated with BoNT long enough to play a role in intestinal absorption has become a controversial topic. There are reports that suggest BoNT will be fully released from the NAPs in the small intestine, and evidence

that the BoNT is capable of crossing the epithelial barrier without them [77,176,177]. The identity of the BoNT receptor on the epithelial surface in the intestine is unknown, but there is evidence to suggest that it differs from the protein receptors used on neuronal cells [178]. There are also reports suggesting that the NAPs contribute to absorption in the intestine [179]. These include experiments in pH 7 rat intestinal juices where the PC does not disassociate [180], or demonstrations that PCs are absorbed by the intestine during various rat ligation duodenum loop assays [181,182].

There is growing evidence that suggests the HA proteins may contribute to intestinal absorption by enhancing adhesion of the BoNT PC to mucins or the cell surface, disrupting the epithelial barrier, or facilitating transcytosis. The crystal structures of the HA1 proteins from serotypes /A, /B, /C, and /D have recently been determined. Every structure except for the /D serotype was co-crystallized with a form of carbohydrate moiety including galactose, lactose, N-Acetyl-D-lactosamine, N-acetylneuraminic acid, or N-acetylgalactosamine [183–185]. The co-crystal structures of the HA3 proteins from serotypes /A and /C with α2-3, α2-6-sialylated oligosaccharides were also recently determined [183,186]. These HA1 and HA3 binding sites could represent points of contact between the BoNT PC and mucins, glycolipids, or glycoproteins in the intestine. Needless to say, the functional role of the HA proteins in the BoNT PC will require more study.

When I initiated this study there was very little known about the actual organization of the BoNT PC. There were crystal structures of assorted NAPs and an array of structural predictions based on biochemical assays. The oral toxicity associated with the BoNT PC suggests an effective protein assembly capable of protecting a protein during passage through the harsh conditions encountered in the gastrointestinal tract and then directing it to specific cell types. Understanding how these proteins assemble to achieve these results has the potential to improve the design and function of many mucosal vaccines or the intestinal absorption of oral biologics. A second structural unknown in the CNT field has been the lack of the TeNT holotoxin structure. It is unclear if its three domains resemble the organization of its BoNT homologues and if so whether it is similar to BoNT/A or BoNT/E or if its structure is unique. A better understanding of the complete structure of TeNT may help explain its trafficking differences from BoNT and may provide new approaches in drug design for neurological disorders.

I have sought to address these gaps in our structural knowledge for the BoNT PC and TeNT using negative stain electron microscopy (EM) and single particle averaging. In Chapter II of this thesis, I describe work done to image the PC assembly for the three BoNT serotypes responsible for human botulism. I was able to describe their molecular assembly using 3D reconstructions of each PC using the random conical tilt method as well as docking the NAP crystal structures into the models. In Chapter III of this work, I describe work done to

explore the structure of the TeNT holotoxin using negative stain EM and single particle averaging. I have been able to show that activation of TeNT does not result in a dramatic conformation change and that its overall structure does not resemble that of BoNT/A.

CHAPTER II

MOLECULAR ASSEMBY OF BOTULINUM NEUROTOXIN PROGENITOR COMPLEXES

Introduction

Botulinum neurotoxin (BoNT) is produced by various strains of *Clostridium botulinum*, *C. butyricum*, and *C. baratii* and is the most potent toxin known. BoNT's are classified into 7 serotypes (A–G) based upon serotype-specific antibody neutralization, and DNA sequencing has revealed multiple subtypes within each serotype [29]. The BoNT's are synthesized as single-chain proteins that are proteolytically cleaved into di-chain proteins, consisting of a 50 kDa light chain (LC) and a 100 kDa heavy chain (HC) [122]. The HC binds receptors on the pre-synaptic neuron in the neuromuscular junction and directs the LC into the neuronal cell cytosol. The LC is a zinc metalloprotease that cleaves components of the synaptic membrane fusion complex and blocks neurotransmitter exocytosis [144]. This inhibition of acetylcholine release in neuromuscular junctions results in the flaccid paralysis associated with botulism.

In adults, the most common form of botulism results from ingestion of BoNT contaminated food, while in infants, the disease typically results from *C. botulinum* colonization and *in situ* BoNT production in the gut [187]. In the case of food contamination, BoNT has to survive passage through the low pH

environment of the stomach. In both cases, BoNT must resist protease degradation in the intestine, cross the epithelial barrier of the digestive tract, and gain access to the nerve ending targets through the blood and lymph circulatory systems [188].

To maintain the activity of BoNT under these conditions, organisms that produce BoNT also produce one or more neurotoxin associated proteins (NAPs) that non-covalently associate with the neurotoxin to form progenitor complexes (PCs) [30]. The PCs have been shown by ultracentrifugation to adopt three sizes: 12S (M-PC, ~ 300 kDa), 16S (L-PC, ~500 kDa), and 19S (LL-PC, ~900 kDa) (reviewed in [30]). The genes for the neurotoxin and its NAPs are located in the same locus (Fig. 2-2a) [38]. The NAPs include three hemagglutinin (HA) proteins (HA1, HA2, and HA3, named for their capacity to agglutinate red blood cells) and a non-toxic, non-hemagglutinin protein (NTNH). Type A2, E, and F strains do not have the HA genes and only produce the 12S PC, a noncovalent complex of BoNT and NTNH. Type B, C, and D strains produce the 12S and 16S PCs. The 16S PC includes BoNT, NTNH, HA1, HA2, and HA3. Type A1 strains produce 12S, 16S, and 19S PCs. The 19S PC may represent a dimer of 16S complexes.

The oral median lethal dose (MLD$_{50}$) of BoNT decreases as the size of the PC increases, suggesting that the NAPs play a role in promoting BoNT passage through the gastrointestinal tract [62,63,189]. A recent structure of a 12S complex shows how BoNT/A1 and NTNH/A1 bind each other in an interlocked complex

that protects the BoNT from acidic and proteolytic degradation (Fig. 2-2a) [47]. But, the role of the NAPs in promoting transport through epithelial cells is more controversial. While the NAPs do not appear to effect the transport efficiency of iodinated BoNT in transcytosis experiments [77,176], experiments in a guinea pig model suggest that only the 16S form of the BoNT/C PC is absorbed from the intestine and released into the serum [190]. Mechanisms for how the HA proteins could enhance intestinal absorption involve their capacity to bind mucins [118,191], bind intestinal microvilli [192], and disrupt the paracellular barrier [193]. Crystal structures of HA1 and an HA3 trimer in complex with carbohydrates reveal sites where these molecules could bind mucins and sialylated gangliosides and/or glycoproteins of the epithelial cell surface [185,186].

Despite these observations, there is limited information regarding the architecture of the BoNT 16S and 19S PCs. A two-dimensional (2D) electron crystallography study of the BoNT/A1 19S PC suggested features with trigonal symmetry [194], and individual electron microscopy (EM) micrographs of the BoNT/D 16S PC suggested that the complex has three extended 'arms' [195]. Here, we have generated 3D reconstructions of the BoNT/A1, /B, and /E PCs, building on a series of 2D class averages obtained by single particle EM and the random conical tilt (RCT) approach [196].

Methods

Specimen Preparation and EM

The BoNT/A1, /B, and /E PCs were purified by List Biological Laboratories and stored in lyophilized form. The purity of the BoNT/A1 and /B PC at the time of purification is indicated by SDS- and Native gels (Fig. 2-1) The samples were hydrated with water to yield solutions that were 0.1 mg/mL protein, 20 mM HEPES pH 6.8 and 1.25% lactose. The samples were further diluted to 50 μg/mL in 20 mM HEPES pH 6.8. Uranyl formate (0.7% wt/vol) was used for conventional negative staining as previously described [197]. Images of the BoNT/A, /B, and /E progenitor complexes were recorded using a Tecnai F20 electron microscope (FEI) equipped with a field emission electron source and operated at an acceleration voltage of 200kV. Images were taken under low-dose conditions at a magnification of 67,000X using a defocus value of -1.5 µm. Images were recorded on a Gatan 4K x 4K CCD camera. Images were converted to mixed raster content (mrc) format, and binned by a factor of 2, yielding final images with a 3.5 Å/pixel. Particle images of the tilted and untilted BoNT/A, /B, and /E PCs were selected and analyzed using SPIDER and the associated display program WEB [198].
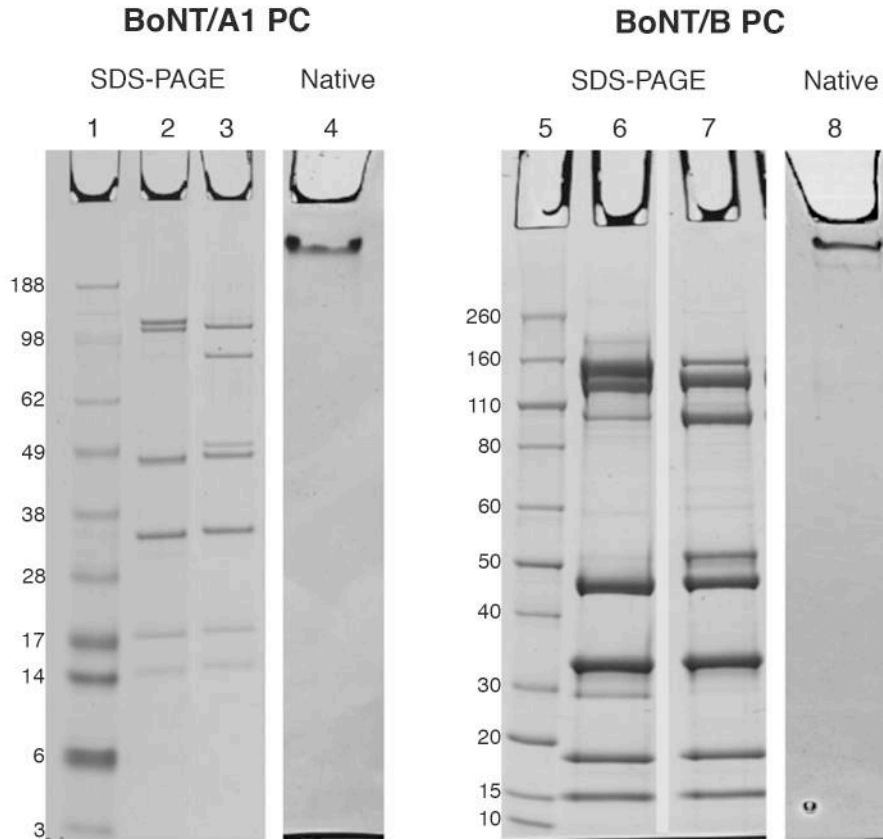
Fig. 2-1. Analysis of the BoNT/A1 and BoNT/B 16S PCs by SDS- and Native-PAGE. Lanes 2 and 6 correspond to non-reducing conditions. Lanes 3 and 7 correspond to reducing conditions. Lanes 4 and 8 were run in the absence of SDS and reductant.

Random Conical Tilt Reconstruction of Negatively Stained BoNT/A, /B, and /E PCs

Micrograph tilt pairs of BoNT/A, /B, and /E PCs were recorded at -55° and 0°. Particle pairs (BoNT/A-PC: 15,507, BoNT/B-PC: 11,765, and BoNT/E-PC: 7,792) were selected interactively from both the tilted and untilted images using WEB and windowed into 120 x 120-pixel images (3.5 Å/pixel). The untilted images were rotationally and translationally aligned and subjected to 10 cycles of

multi-reference alignment and K-means classification using no designated initial reference.

BoNT/A PC

Particles were grouped into 4, 5, 25, 50, 75, 100, 200, and 300 classes. An initial 3D reconstruction was done using the titled particles (2,550) associated with one average from the five group classification (Fig. 2-2, black star). The initial 3D reconstruction was done by back-projection using the in-plane rotation angles determined by rotational alignment and the preselected tilt angle of 55° implemented in the processing package SPIDER. To increase the number of particles included in the 3D reconstruction, 5,019 tilted images plus 500 nontilted images associated with a class average in the 4-group alignment (Fig. 2-5b) were used to further refine the structure using angular refinement in SPIDER. Using a FSC = 0.5 criteria the resolution is ~15 Å (Fig. 2-5a); however, the lack of any secondary structural details in our map suggests that the resolution more likely falls closer to 20 Å.

12 classes were selected from the class average of 50 for additional multi-reference alignment (Fig. 2-6, black dots). A class of 1,114 particles showing a 'prong' orientation (Fig. 2-5c, black star) was used to calculate an initial 3D reconstruction by back-projection using the same variables described above. The resulting density map was used for the back-projection and angular refinement in SPIDER. Ten percent of the untilted particles were included in the data set (115

42

particle images) and angular refinement was repeated. Using a FSC = 0.5 criteria, the resolution is ~15 Å (Fig. 2-3b); however, examination of structural features in the density map suggests the resolution is closer to 20 Å or higher.
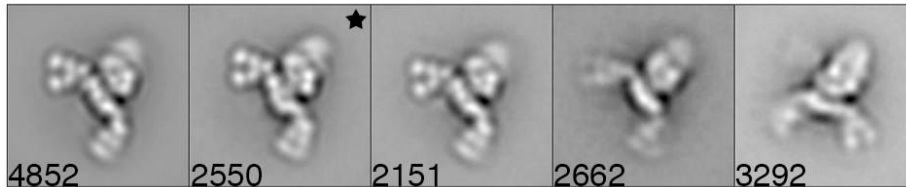
Fig. 2-2. The BoNT/A1 PC sorted into five classes. The tilted particles associated with the average marked with "★" were used for an initial 3D reconstruction by back projection of the two-armed complex shown in Fig. 3c. Side length of panels, 420 Å.
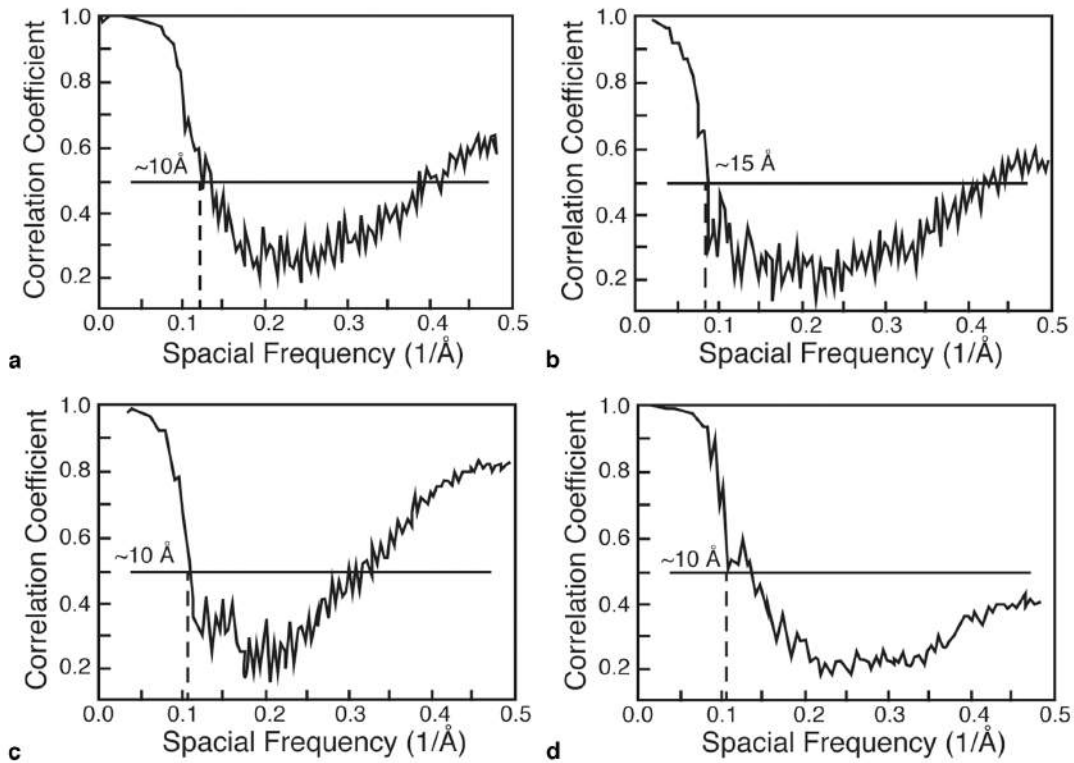
Fig. 2-3. The Fourier shell correlation (FSC) curve for (a) the BoNT/A1 PC 'flat' view reconstruction from Fig. 2-4a, (b) the BoNT/A1 PC 'prong' view reconstruction from Fig. 2-4b, (c) the BoNT/B reconstruction from Fig. 2-5b, and the BoNT/E reconstruction from Fig. 2-6b.

BoNT/B PC

Particles were grouped into 75 classes. 19 classes were selected from the class average of 75 for additional multi-reference alignment (Fig 2-11, black dots). A class of 2,614 particles (Fig. 2-10a, black star) was used to calculate an initial 3D reconstruction by back-projection using the same variables described above. The resulting density map was used for the back-projection and angular refinement in SPIDER. Ten percent of the untilted particles were included in the data set (260 particle images) and angular refinement was repeated. Using a

44

FSC = 0.5 criteria, the resolution is ~15 Å (Fig. 2-3c); however, the lack of any secondary structural details in our map suggests that the resolution more likely falls closer to 20 Å. The FSC curves for BoNT/A1 and /B PCs do not stay close to zero at high resolutions of the graph. We attribute this to artifacts created by the large amount of noise present from the flexible third "arm" that could not be resolved in the maps.

BoNT/E PC

Particles were grouped into 10 classes using reference free alignment. Four classes were selected as references for an additional round of multi-reference alignment (Fig. 2-12, black dots). A 3D structure was calculated using back-projection from the titled images associated with a class of 692 particles from the initial alignment (Fig. 2-12, black star) as an initial model for angular refinement of 4,518 tilted images plus 450 nontilted images from a class generated in the reference-based alignment (Fig. 2-11, black star). Using a FSC = 0.5 criteria, the resolution is ~15 Å (Fig. 2-3d); however, the lack of any secondary structural details in our map suggests that the resolution more likely falls closer to 20 Å.

The contouring threshold for all structures was chosen so that the volume of the structure was continuous. For display purposes structures were filtered in chimera [199] using the "Hide Dust" command to diminish 'salt and pepper' noise

from the maps by removing single voxels that were unconnected to the main volume of the 3D density.

Negative Staining of an Antibody-BoNT/A PC complex

The 4LCA antibody was purified as previously described [200]. For antibody labeling, the proteins were mixed in 1:10 molar ratios and incubated at room temperature for 3 h before grid preparation. Grids were prepared as described [197]. 403 particles of BoNT/A PC bound to 4LCA were selected interactively using WEB and windowed into 150 x 150-pixel images (3.5 Å/pixel). The images were rotationally and translationally aligned and subjected to 10 cycles of multi-reference alignment and K-means classification with no initial references designated.

Results

Visualization of BoNT PCs by negative stain EM

BoNT/A1, /B, and /E PC were adsorbed to carbon-coated glow-discharged grids and stained with uranyl formate. EM micrographs revealed monodisperse macromolecular assemblies suitable for additional structural analysis for all three serotypes. Examination of BoNT/A1 and /B PCs revealed particles composed of an ovoid-shaped 'body' attached at one side to three extended 'arms' (Fig. 2-4b, 2-4c, 2-5a, 2-10a). Although BoNT/E PC particles shared the same ovoid-shaped

body, they lacked the extended arms (Fig. 2-4d). To more closely examine the

organization of PC complexes, image pairs of BoNT/A1, /B, and /E were

collected so that the 3D structure of each serotype could be determined using the

RCT approach.
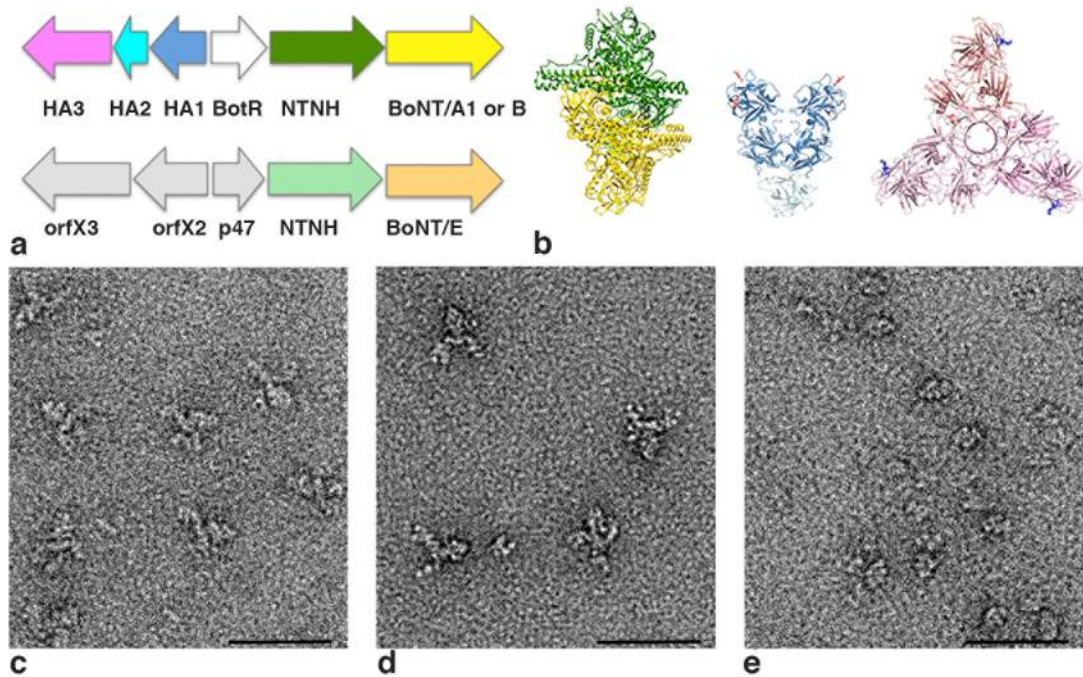
Fig. 2-4. The BoNT PC is comprised of the neurotoxin and NAPs. (a) The BoNT gene locus for representative strains expressing BoNT serotypes /A1, /B, and /E. Shown below are the crystal structures for the BoNT/A1-NTNH complex (3V0A), the BoNT/D (HA1)$_2$-HA2 trimer (2E4M), and the BoNT/C HA3 trimer (4EN6). The structures are colored to match the colors in the gene locus such that BoNT/A1 is yellow, NTNH is green, HA1 is blue, HA2 is light blue, and HA3 is pink. Two N-acetylgalactosamine binding sites have been identified in the structure of HA1/C (3AH2 and 3AJ6), and the sugars have been superimposed on the BoNT/D (HA1)$_2$-HA2 trimer structure and depicted as red sticks. The HA3 trimer was crystallized with alpha 2-3-sialyllactose which is depicted in blue sticks. (b) The BoNT/A1 PC has three arms projecting away from an ovoid body. (c) The BoNT/B PC has a similar structure to the /A1 complex. (d) The BoNT/E PC is smaller and resembles the ovoid body seen in the /A1 and /B PCs. (Scale bar in images b-d, 50 nm.)

The BoNT/A1 PC is a flexible three-armed structure

Image pairs of grids containing negatively stained BoNT/A1 PC were recorded at tilt angles of -55° and 0°. A total of 15,507 pairs of particles were selected, and images of the untilted specimens were classified into four class averages (Fig. 2-5b). Each class revealed a 'pincher-like' feature at the end of the arms; however, unlike the raw images that clearly showed particles with three extended arms (Fig. 2-4b, 2-5a), only two arms were visible in the averages (Fig. 2-5b). To attempt to resolve the third arm apparent in our raw images, we expanded the number of classes to 50 (Fig. 2-6).
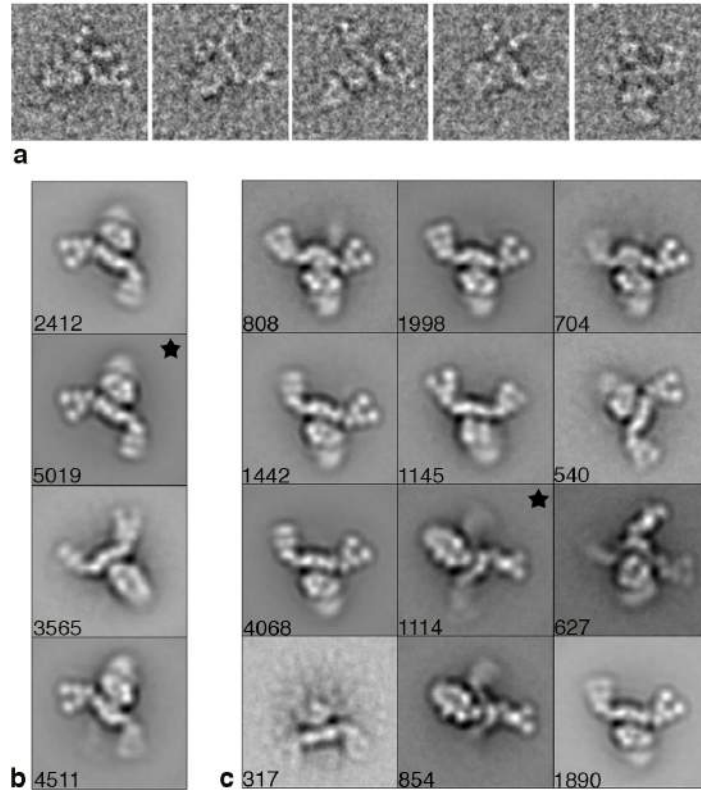
Fig. 2-5. The BoNT/A1 PC is a flexible three-arm structure. (a) The three arms are evident in a gallery of single particles. (b) When 15,507 particles are sorted into four classes only two arms of the PCs three arms are visible. The box marked with "★" indicates the "flat" view class used for a 3D reconstruction. (c) BoNT/A1 PC class averages obtained by reference-based alignment. The box marked with "★" indicates the class used for an alternate "prong" view 3D reconstruction. Side length of panels, 420 Å.

As expected, when the particles were sorted into a larger number of classes, we began to observe averages containing three arms, although one of the three arms was always less resolved than the other two. In addition, from this group of 50 class averages we noticed that the particles adsorb to the carbon film in two distinct orientations. One is a 'flat' orientation that is composed of an ovoid body with two well-defined arms (Fig. 2-6, black star) and the other is a 'prong' orientation that contains an ovoid body with only one well-defined arm (Fig. 2-6,

white star**). A majority of the averages (containing ~90% of the total particles) are in the 'flat' orientation, while the remaining averages (containing ~10% of the total particles) are in the 'prong' orientation. To generate better resolved 'prong' averages we selected 12 class averages from our analysis using 50 classes (Fig. 2-6, black dots) and used these for a further round of reference-based alignment (Fig. 2-5c).
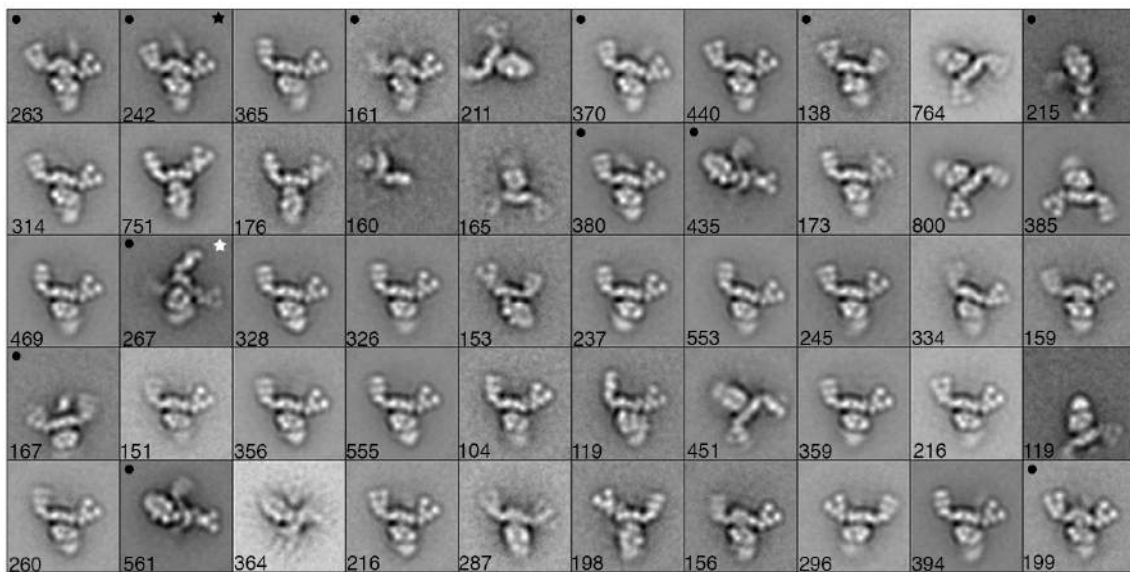
Fig. 2-6. Classes of BoNT/A1 PC three-armed species begin to emerge if the class size is expanded to 50. The two preferred orientations of the PC on the grid surface are indicated by either a black "★" ('flat' view) or by a white "★" ('prong' view.). Boxes marked with "•" indicate classes selected for the referenced-based alignment shown in Fig. 2. Side length of panels, 420 Å.

In an effort to generate averages containing an ovoid body with three well–resolved arms, the particles were sorted into groups of 100, 200, or 300 classes. When divided into 300 classes, the third arm is visible in a third of the class averages; however each class contains only a small number of particles making the averages noisy and not suitable for 3D reconstructions. When comparing

distinct classes composed of particles either in the 'flat' or 'prong' view, it is clear there is significant flexibility in the orientation of the pinchers relative to the arms and the orientation of the arms relative to the ovoid body and suggests that flexibility is an intrinsic feature of the BoNT/A1 PC.

The conformational heterogeneity made it difficult to generate well-populated classes containing three well-resolved arms. Therefore, we opted to calculate two 3D reconstructions using tilted images either associated with a class average in the 'flat' orientation (Fig. 2-5a, black star) or associated with a class average in the 'prong" orientation (Fig. 2-5b, black star) using the RCT approach. Both reconstructions led to well-defined 3D structures that contained features seen in the 2D averages (Fig. 2-7a and b), suggesting that the 3D reconstructions were successful. The overall features of the structure generated from the 'flat-view' particles (Fig. 2-7a) are better resolved than the features seen in the structure generated from the 'prong-view' particles (Fig. 2-7b). This is due to the larger number of images in the 'flat' projection average (5,019) than in the "prong" projection average (1,114). We aligned our two 3D reconstructions ('flat' and 'prong' structures) to produce a 3D model of the three-armed BoNT/A1 PC (Fig. 2-7c). Our model shows a triangular plate and V-shaped pinchers assembled at one end of an ovoid-shaped body and agrees well with the three-armed complex we observe at the single particle level in our EM micrographs (Fig. 2-5a).
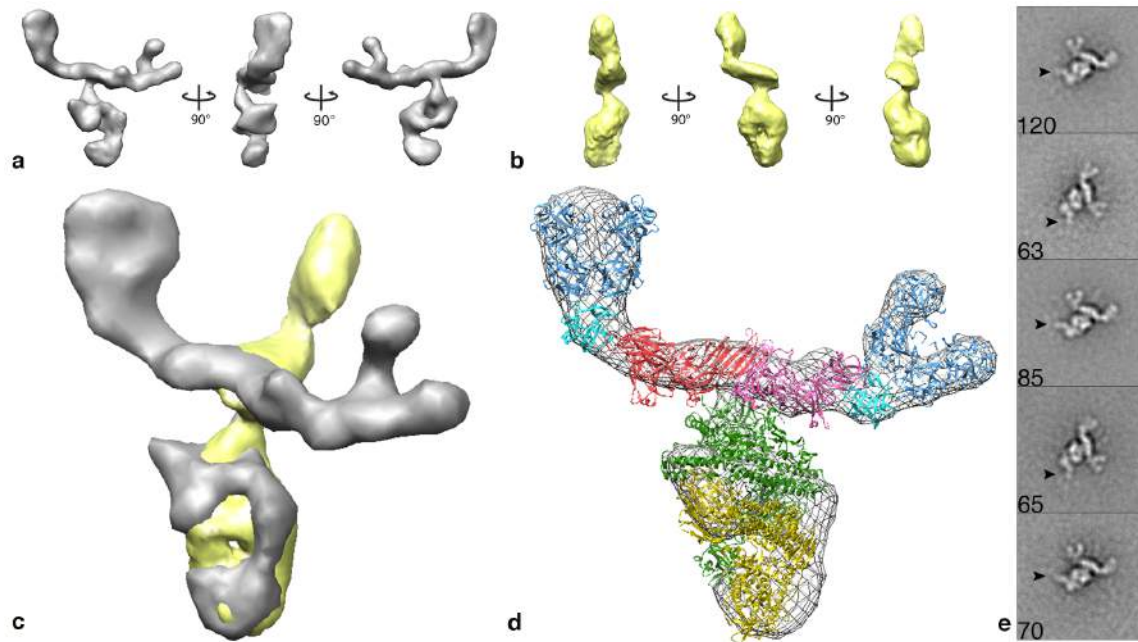
Figure 2-7. The molecular organization of the BoNT/A1 PC. (a) Surface representations of 3D reconstructions of the BoNT/A1 "flat" view and (b) "prong" view in negative stain. (c) An alignment of the two BoNT/A1 3D views reproduces the three-armed complex observed in our EM micrographs. (d) Crystal structures (from Fig. 1a) placed into a mesh representation of the "flat" view reconstruction. (e) Class averages of the BoNT/A1 PC with an antibody specific to the neurotoxin's catalytic domain reveal specific binding at the end of the ovoid body furthest away from the HA proteins (black arrows). The scale bars for images a-d correspond to 50 Å.

The observed geometric features of ovoid body, triangular plate, and V-shape pinchers correlate with the shapes observed in the high-resolution crystal structures of the BoNT/A1-NTNH complex [47], the BoNT/C HA3 trimer [193], and the BoNT/D $(HA1)_2$-HA2 trimer [195], respectively (Fig. 2-4a, 2-7d). While the EM structure is not at a resolution that would permit a detailed docking analysis, the BoNT/D $(HA1)_2$-HA2 trimer could easily be placed into the 'pinchers' and the BoNT/C HA3 trimer was placed into the triangular plate of the electron density map. The orientation of the BoNT/C HA3 trimer was guided by the fact

that the BoNT/C HA3 proteins, when viewed from the side, form a shallow 'W' shape consistent with features we observe in our structure (Fig. 2-8). While it was clear that the remaining ovoid body corresponded to the BoNT/A1-NTNH complex, there were two possible ways to orient the crystal structure of the complex within our density map. The genes encoding BoNT/A1 and NTNH are thought to have emerged from a gene duplication event, and the structures of these two molecules are similar [47]. In one scenario, the BoNT/A1 LC would make contact with the HA3 triangular plate while the LC-equivalent of the NTNH (nLC) would form the base of the ovoid body. In the other scenario, the nLC would be in contact with the HA3 trimer while the BoNT LC was at the distal end of the complex. To distinguish between these two possibilities, we labeled the PC with a BoNT/A1 LC specific monoclonal antibody [200]. We observed consistent and efficient labeling of the distal end of the ovoid body (Fig. 2-7e, 2-9) thus confirming the placement where the nLC interacts with the HA3 trimer. The placement of the crystal structures (Fig. 2-4a) into the two arm and three arm structures of the BoNT/A1 PC is shown in Figures 2-7d and 2-10, respectively.
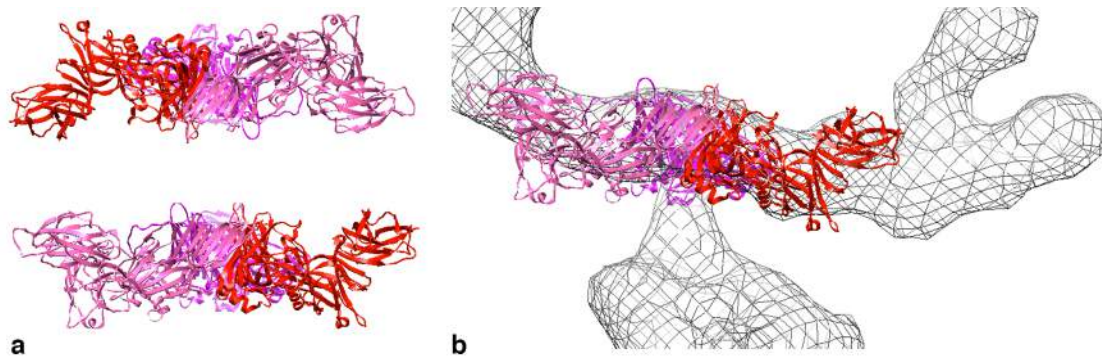
Fig. 2-8. Orienting the HA3 trimer in the PC structure. (a) When viewed from the side, the HA3 trimer adopts either a 'M' or 'W' shape. (b) When the electron density is oriented with the pinchers at the top and the ovoid body at the bottom, the HA3 trimer can be confidently placed into the triangular plate in the 'W' orientation. The scale bar corresponds to 50 Å.
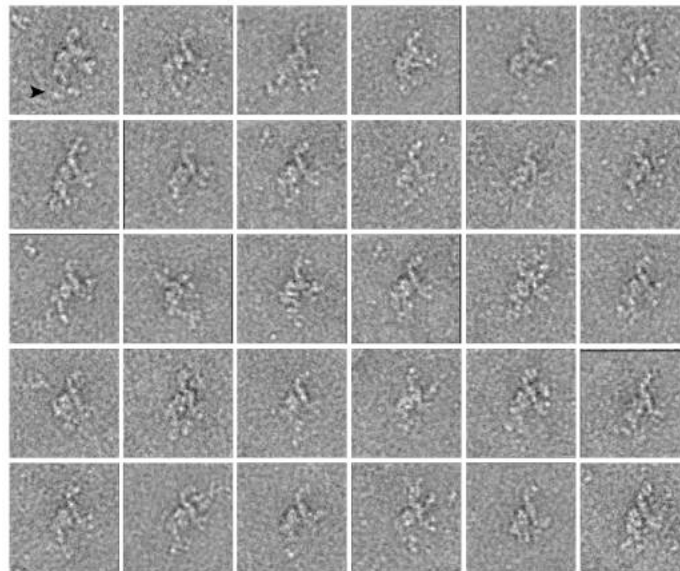
Fig. 2-9. Labeling the BoNT/A1 PC with an antibody against the neurotoxin's catalytic domain. The BoNT/A1 complex was incubated with 4LCA and visualized by negative stain EM. A gallery of labeled single particle BoNT/A1 PCs is shown. Side length of panels, 525 Å.

The BoNT/B PC has a similar structure to the BoNT/A1 PC

Negative stain EM micrographs of the BoNT/B PC show a macromolecular assembly that closely resembles the BoNT/A1 PC (Fig. 2-4c, 2-10a) although the sample appeared to be more heterogeneous with PC assembly or disassembly intermediates evident as single particles. Image pairs were collected at tilt angles of -55° and 0° and a total of 11,765 particles were selected. The untilted particles were initially sorted into 75 classes and averaged (Fig. 2-11). In addition to a 'flat' view, similar to what we observed with the BoNT/A1 PC, we observed complexes where one or more of the components seemed to be missing (Fig. 2-11, colored boxes). 19 classes representing the range of complexes observed in the sample were selected for multi-reference alignment (Fig. 2-11, black dots). A class containing 2,614 particles that clearly showed the main body with two of the three arms well-resolved was selected for 3D reconstruction (Fig. 2-10b, black star). The face view of the density map closely resembles the projection map suggesting a successful 3D reconstruction (Fig. 2-10c). The overall BoNT/B PC reconstruction resembles that of the BoNT/A1 PC. Independent placement of the crystal structures (Fig. 2-10d) suggests that the BoNT/A1 and BoNT /B PCs have a similar structural organization.
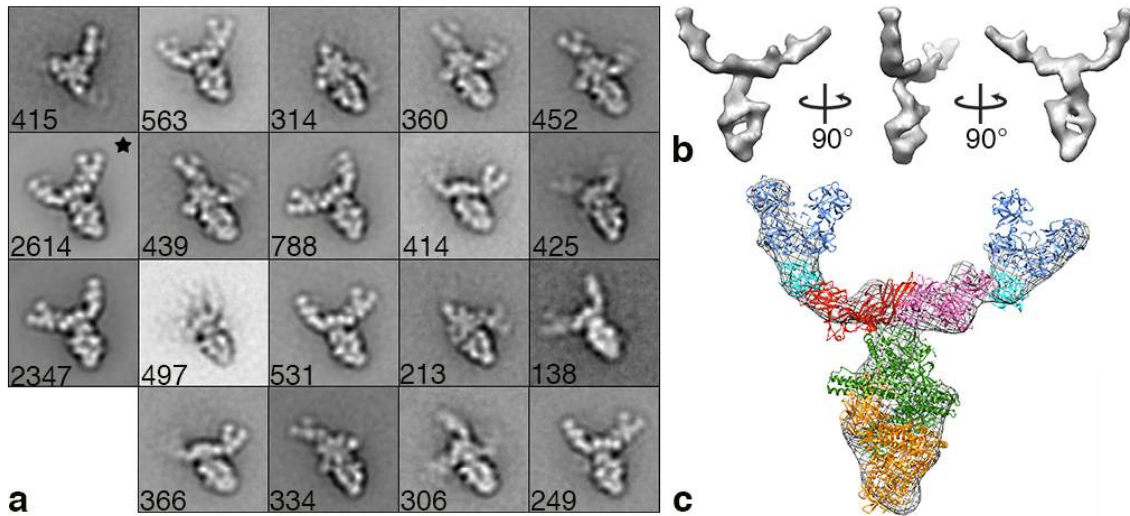
Fig. 2-10. The BoNT/B PC has a similar structure to the BoNT/A1 PC. (a) The three arms are evident in a gallery of single particles. (b) BoNT/B PC class averages obtained by reference-based alignment and classification. The box marked with "★" indicates the class used for the 3D reconstruction shown in c and d. Side length of panels in a and b, 420 Å. (c) Surface representation of the 3D reconstruction of BoNT/B PC. (d) Crystal structures (from Fig. 2-2a) placed into a mesh representation of the BoNT/B PC. The scale bars in panels c and d correspond to 50 Å.
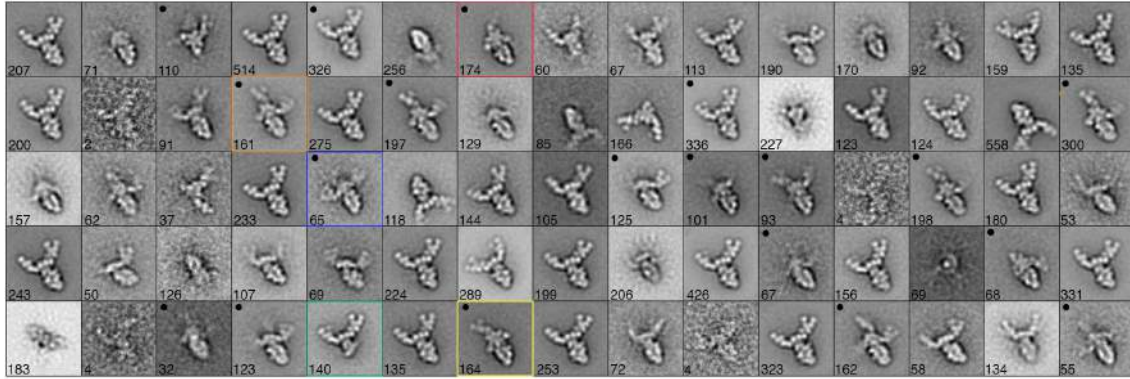
Fig. 2-11. The BoNT/B PC sample contains assembly/disassembly intermediates. Boxes marked with "•" indicate classes selected for the referenced-based alignment shown in Fig. 4a. The outlined boxes show different assembly/disassembly states in the sample: red = no HA1/HA2 pinchers, yellow = one pair of pinchers, orange = two pairs of pinchers, blue = three pairs of pinchers, and green = the NAP assembly without the neurotoxin. Many of the classes with two pairs of pinchers (including the one in orange) also include individual particles with 3 pinchers where the third pincher has not been resolved due to flexibility. Side length of panels, 420 Å.

The BoNT/E PC resembles the ovoid body observed in the BoNT/A1 and BoNT/B complexes

Negative stain EM micrographs of the BoNT/E PC show a macromolecular assembly that closely resembles the ovoid-shaped body observed in the BoNT/A1 and BoNT/B PCs (Fig. 2-4d). The smaller particles are consistent with the description of BoNT/E PC as a 12S complex and the fact that the BoNT/E gene locus does not have the HA operon. Image pairs were collected at tilt angles of -55° and 0° and a total of 7,792 particles were selected. The untilted particles were sorted and averaged in 10 classes (Fig. 2-12) and reveal classes resembling the ovoid body of the BoNT/A1-NTNH/A1 complex and classes that likely represent dissociated BoNT/E or NTNH/E monomers. Four classes were selected for multi-reference alignment (Fig. 2-12, black dots). A referenced-based

alignment class containing 4,518 particles that clearly showed the ovoid body was selected for a 3D reconstruction (Fig. 2-13a, black star). The face view of the density map resembles the projection map suggesting a successful 3D reconstruction (Fig. 2-13b). We could not unambiguously place the BoNT/A1 12S PC crystal structure into the 3D reconstruction of the BoNT/E 12S PC, because we lacked an antibody that could be used to determine which end corresponded to the BoNT/E LC and which end corresponded to the nLC of NTNH/E. However, the symmetry of the BoNT/E 12S structure (Fig. 2-13b) and the similarity with the ovoid bodies observed in the structures of the BoNT/A1 (Fig. 2-7a, 2-7c) and BoNT/B (Fig. 2-10c) PCs suggest that BoNT/E is capable of binding NTNH/E in a conformation similar to how BoNT/A1 binds NTNH/A.
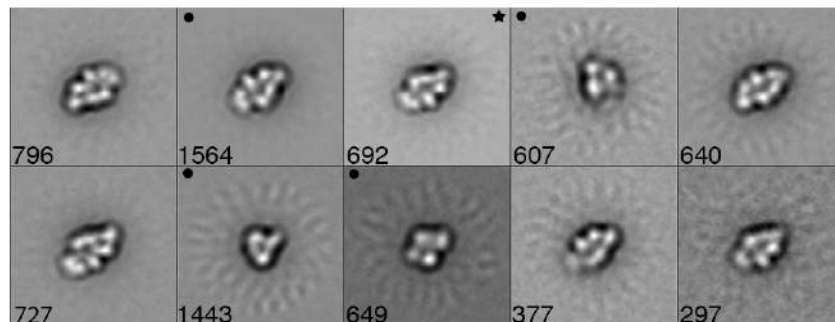
Fig. 2-12. A BoNT/E PC class average of 10 shows the two-protein complex and individual proteins likely from the complex. Boxes marked with "•" indicate classes selected for the referenced-based alignment shown in Fig. 5a. Side length of panels, 420 Å.

58
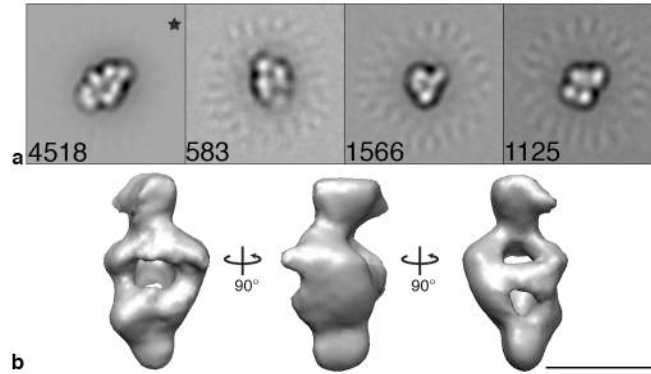
Fig. 2-13. The BoNT/E PC resembles the ovoid body observed in the /A1 and /B PCs. (a) BoNT/E class averages obtained by reference-based alignment and classification. The box marked with "★" indicates the class used for the 3D reconstruction shown in b. Side length of panels, 420 Å. (b) Surface representation of the 3D reconstruction of the BoNT/E PC. The scale bar corresponds to 50 Å.

Discussion

Our study provides the first 3-D descriptions of the BoNT/A1 16S PC, the BoNT/B 16S PC and the BoNT/E 12S PC. Our data suggest that the BoNT/A1 PC adopts a flexible three-armed structure with a BoNT:NTNH:HA1:HA2:HA3 stoichiometry of 1:1:6:3:3. A BoNT/A1 PC with this stoichiometry has a calculated MW of ~760 kDa, halfway between the estimates provided by centrifugation studies (500 kDa for the 16S PC and 900 kDa for the 19S PC). The BoNT/A1 PC structure (Fig. 2-7a and 2-7d) resembles the BoNT/B PC structure (Fig. 2-10c and 2-10d) as well as the model put forth by Hasegawa *et al.* based on electron micrographs of the BoNT/D PC [195]. We interpret this similarity to mean that the BoNT/A1 PC structure is in the 16S form. No evidence of dimers or larger

59

complexes was observed in our analysis of the BoNT/A1 PC sample and could reflect dissociation of the 19S PC at low concentrations [173].

In addition to dissociation of the 19S complex, there are reports that document the reversible assembly and disassembly of components in the smaller complexes [201,202]. We observed this in our analysis of the BoNT/B PC sample which had structures resembling the 1) BoNT-NTNH ovoid body 2) BoNT-NTNH bound to an HA3 trimer, or 3) BoNT-NTNH-(HA3)$_3$ associated with either 1, 2, or 3 (HA1)$_2$-HA2 assemblies (Fig. 2-10a). *In vitro*, the complexes are known to be pH-sensitive, with disassembly occurring at pH $\geq$ 7.5 [171,172,203]. What occurs in the context of the small intestine is less clear. Some reports suggest that the BoNT will be fully released from the NAPs in the small intestine (the pH of the duodenum is ~ 7.0), and there is evidence documenting the capacity of the BoNT to cross the epithelial barrier in the absence of the NAPs [77,176,177]. Experiments in pH 7 rat intestinal juices however, indicate that the PC does not dissociate [180]. Whole PCs are capable of being absorbed from the intestine into the lymphatics in a rat ligated duodenum loop assay [181], consistent with the hypothesis that the NAPs contribute to absorption in the intestine [179].

There are now strong data to support the role of NTNH in protecting the BoNT from acidic and proteolytic degradation in the digestive tract [47]. These data are consistent with the 10-20x enhancement in oral MLD$_{50}$ when the 12S PC is compared to the neurotoxin alone [62]. We know that the addition of the HA

60

proteins to form the larger 16S PC enhances the oral MLD_{50} even further (the BoNT/A1 16S PC is 1.6x more potent than the BoNT/A1 12S PC and the BoNT/B 16S PC is 733x more potent than the BoNT/B 12S PC) [62]. Our structures of the BoNT/A1 and BoNT/B 16S PCs indicate that the HAs have no direct contact with the BoNT's, and suggest that the HAs do not play a 'protective' role but instead contribute to intestinal absorption.

The HA proteins could contribute to intestinal absorption by enhancing adhesion of the BoNT PC to mucins or the cell surface, disrupting the epithelial barrier, or by facilitating transcytosis [179]. Consistent with the capacity of the HAs to agglutinate red blood cells, the HAs are known to bind a variety of sialylated oligosaccharides. Binding studies using a glycoconjugate microarray indicate that HA3/C preferentially recognizes a2-3- and a2-6 sialylated sugars, and the binding site for these sugars has been elucidated by X-ray crystallography [186] (Fig. 2-14b). N-acetylneuraminic acid, N-acetylgalactosamine, and galactose block the binding of HA1/C to mucins, and crystallography has revealed a common site where these sugars can bind. Galactose is also capable of binding a second site on HA1/C [185]. These binding sites could represent points of contacts between the BoNT/C PC and mucins, glycolipids, or glycoproteins within the intestine. While co-crystal structures of the HAs from /A1 and /B strains with sugars are not yet available, the HA molecules share a high degree of sequence identity at the amino acid level suggesting that the sugar binding sites could be conserved. Importantly,

each binding site is accessible in the models we have generated of the BoNT/A1 and BoNT/B 16S PC (Fig. 2-14a, 2-14d, 2-14e).

The BoNT's are also known to interact with sialic acid containing sugars, and the interaction with G_{T1b} gangliosides are known to be important in the dual-receptor model where BoNT uses a ganglioside and protein to mediate interaction with the neuronal cell surface [204]. The G_{T1b} binding pocket has been defined by X-ray crystallography [205] and is accessible in the context of the 16S PC structure (Fig. 2-14c, 2-14e). Since G_{T1b} gangliosides are present in epithelial cells of the small intestine, this interaction could contribute to adhesion as well. SV2 and synaptotagmin are, respectively, known protein receptors for BoNT/A1 and BoNT/B on neurons [117,154,206] but the relevance of these receptors in the intestine is not clear. We note that the SytII binding site for BoNT/B [121,155] is fully accessible in the context of the 16S PC structure (Fig. 2-14c, 2-17e).

Our structural studies have shown that the BoNT/A1 and BoNT/B 16S PCs are flexible three-armed structures. The fact that the HA proteins do not interact directly with the BoNT suggests that they are not required for toxin protection but may be important for multivalent binding interactions with mucin and/or the epithelial cell surface. It is tempting to speculate that the flexibility we observed in the analysis of the BoNT/A1 PC allows the complex to effectively 'sample' the intestinal surface and improve the chances of absorption of the toxin prior to high pH dissociation of the complex and proteolytic degradation of the neurotoxin.

The potential to harness the HA proteins as a platform to increase intestinal absorption in other applications is an exciting possibility for future studies.
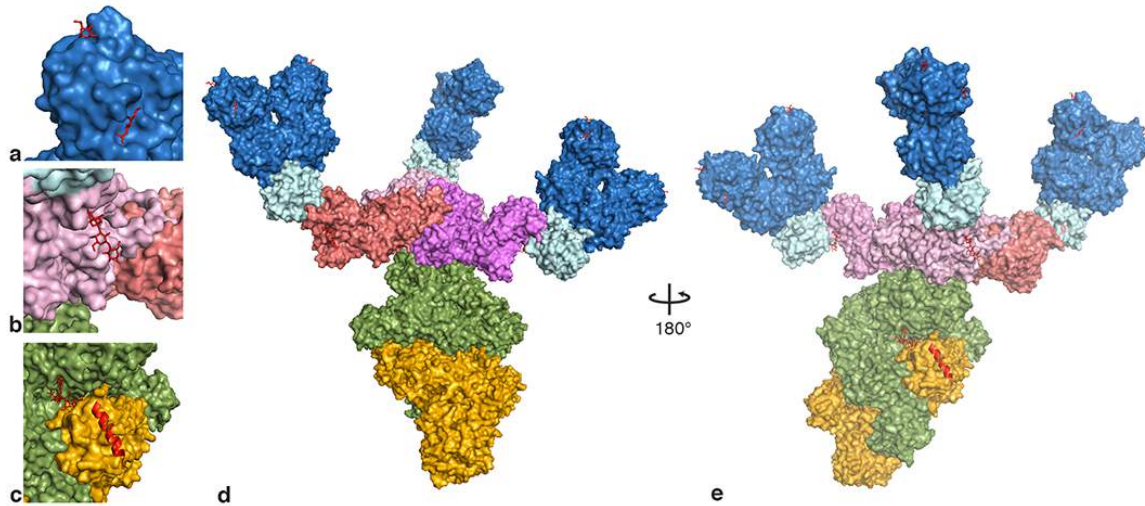
Fig. 2-14. 16S PCs have multiple sugar binding sites. 16S PCs have multiple sugar binding sites. (a) Two N-acetylgalactosamine binding sites have been identified in the structure of HA1/C (3AH2 and 3AJ6), and the sugars have been superimposed on the BoNT/D $(HA1)_2$-HA2 trimer structure (blue) and depicted as red sticks. (b) The HA3 trimer (pink) was crystallized with alpha 2-3-sialyllactose which is depicted in red sticks. (c) The G_{T1b} binding site (with G_{T1b} shown in red sticks) is located between BoNT/A1 (gold) and NTNH (green). Superposition of the BoNT/B HCR-SytII structure (2NM1) onto the BoNT/A1 HCR suggests that the SytII binding site will be accessible in the BoNT/B PC structure (SytII depicted as a red a-helix). (d) A model of a 'flat' view BoNT/A1 PC shown with three arms. (e) The BoNT PC rotated 180 degrees to the 'prong' view reveals the accessibility of the G_{T1b} binding site and the SytII binding site.

Chapter III

ANALYSIS OF TETANUS HOLOTOXIN BY ELECTRON MICROSCOPY

REVEALS NEW INSIGHT INTO ITS STRUCTURAL ORGANIZATION

Introduction

Tetanus neurotoxin (TeNT) is the causative agent of the debilitating spastic paralysis known as tetanus. TeNT is only produced by the anaerobic bacteria *Clostridium tetani*, and is considered the second most potent toxin on the planet after botulinum neurotoxin (BoNT) [27]. *C. tetani* form spores when growth conditions become unfavorable. These spores, which can remain dormant for long periods of time, are widely distributed in the environment and are often found in soil samples [207]. Tetanus can develop after a wound becomes contaminated with *C. tetani* spores. Wounds that offer anaerobic conditions allow the spores to germinate into toxin producing bacteria. TeNT is synthesized as a single-chain polypeptide that is proteolytically cleaved to form an active dichain molecule [208]. The chains consist of a 50 kDa light chain (LC) and a 100 kDa heavy chain (HC) that remain linked by an interchain disulfide bond. The toxin has three ~50 kDa functional domains: binding, translocation, and catalytic. Nicked TeNT has a N-terminal LC linked to the HC, which contains the N-terminal translocation domain (HC_N) and C-terminal binding domain (HC_C). The LC is the catalytic domain of the toxin and functions as a zinc protease that

targets and selectively cleaves the vesicle associated SNARE protein synaptobrevin [144,145].

After entry into the blood stream, TeNT initially targets the presynaptic membrane of peripheral nerve terminals [65]. The HC_N has two carbohydrate binding pockets: a lactose-binding site and a sialic acid binding site which has been shown to bind multiple glycosphingolipids [115,125,209] that are enriched on peripheral nerve terminals. These gangliosides function as dual receptors that bind TeNT HC_C with high affinity [28,125,210]. Upon binding, TeNT undergoes clathrin-dependent, epsin-1 independent endocytosis [128] which allows the toxin to be sorted into an endosomal vesicle that is not acidified [129,133]. The vesicle containing TeNT continues to motor neurons in the spinal cord via a fast axonal retrograde transport that requires F-actin, microtubules, and related motor proteins [131,132]. These findings suggest that this particular endocytic route prevents HC_N membrane insertion and LC release into the cytoplasm thus allowing TeNT to remain intact during its transport [116]. TeNT then crosses intersynaptic space between peripheral motor neurons and inhibitory interneurons. The toxin binds a receptor on the presynaptic membrane of the inhibitory interneuron. The receptors identity is still a matter of debate [124,211]. TeNT enters the neuron via synaptic vesicle and as the pH of this vesicle lowers the conformation of the toxin changes. The HC_N insertion into the endosomal membrane triggers the release of the LC into the neuronal cell cytosol [143]. Here, the TeNT LC selectively targets and cleaves synaptobrevin, a vesicle

associated protein required for the docking and membrane fusion of neurotransmitter synaptic vesicles. Cleavage of synaptobrevin prevents the release of the inhibitory neurotransmitters γ-aminobutyric acid (GABA) and glycine resulting in the uncontrollable motor reflex responses to sensory stimulation that characterize the spastic paralysis of tetanus [212].

TeNT has a ~65% sequence identity with the BoNT serotypes [156] and while the debilitating paralysis associated with TeNT and BoNT are very different, the two proteins share many structural similarities. Both toxins are activated by protease mediated nicking into dichain peptides that remain linked by a disulfide bridge. Furthermore, the heavy and light chains of each toxin are organized into similar functional domains. The crystal structures for the three BoNT serotypes associated with human disease (types A, B, and E) have been determined [146–148]. Interestingly, the *individual* domains for each of the BoNTs have comparable structures though the overall domain organization for the toxins varies. The three domains of BoNT/A and /B are organized such that the catalytic and binding domains are located on either side of the translocation domain. The structure of BoNT/E is unique in that the binding and catalytic domains are located on the same side of the translocation domain (Fig. 3-4b).

The structure of the tetanus holotoxin is currently unknown however, the structures for the TeNT binding and catalytic domains have been determined individually [112,145,149,151] and are similar to their BoNT counterparts. The holotoxin has been crystallized [213–215] but not for the purpose of collecting X-

ray diffraction data. TeNT holotoxin secondary structures have been studied using Fourier transform infrared spectroscopy and circular dichroism [216,217]. A three-dimensional (3D) analysis of the holotoxin was performed using electron crystallography of two-dimensional (2D) crystals bound to a lipid monolayer [218]. The resulting structure is low resolution and described as "mitten shaped" with a "palm" separated from the "thumb" by a pronounced groove.

Despite these structural studies, the organization of TeNTs three domains, how they relate to one another, or how its structure compares to other BoNTs is unknown. Here, we present 2D images of the TeNT holotoxin generated by negative stain electron microscopy (EM) and single particle averaging. The subsequent TeNT images were then compared to the BoNT/A and /E structures. Our analysis shows that TeNT does not undergo a discernible conformation change upon activation and that its holotoxin structure is more similar to BoNT/E than /A.

METHODS

Protein Expression and Purification

Dr. Michael Baldwin, at the University of Missouri, generously provided the wild type TeNT gene in a pET28 expression plasmid. TeNT was recombinantly expressed in *E. coli* BL21-AI cells. Transformed cells were grown in 5 mL luria broth (LB) subculture containing 50mg/L kanamycin at 37°C for ~3 h. When

67

subculture was slightly turbid 200 µL was plated as a lawn on LB agar plates supplemented with kanamycin and grown overnight at 37°C. The bacterial lawn was gently suspended in 10 mL LB and transferred to a 2L flask containing LB supplemented with kanamycin. The cultures were placed at 30°C and 220 rpm. When the cultures reached OD_{600} = 0.6 expression was induced by the addition of $_L$-Arabinose to a final concentration of 0.2% wt/vol and IPTG to a final concentration of 0.75 mM. Incubation was continued overnight at 16° and 220 rpm. After ~18 h the cells were harvested by centrifugation and resuspended in 50 mM NaCl, 30 mM Tris, pH 8.0. Following French Press lysis, the lysates were centrifuged at 39,000xg for 30 min. Protein was purified from the supernatant by Ni^{2+} affinity in 50 mM NaCl, 30 mM Tris, pH 8.0 buffer. TeNT eluted from the Ni^{2+} column with 200 mM imidazole. Ion exchange chromatography was used with 30mM Tris, pH 8.0 buffer that ranged from zero NaCl content to 500 mM. Gel filtration chromatography was the final purification step and was run in 30 mM Tris pH, 8.0, 100 mM NaCl buffer.

Trypsin digestion was used to recapitulate the activated, nicked form of the toxin. TeNT at a concentration of I mg/mL was digested overnight at 4°C with 1 mg/mL trypsin at 1:1000 (Fig. 3-1). This produced dichain molecules that could be separated by disulfide bond reduction (Fig. 3-1).
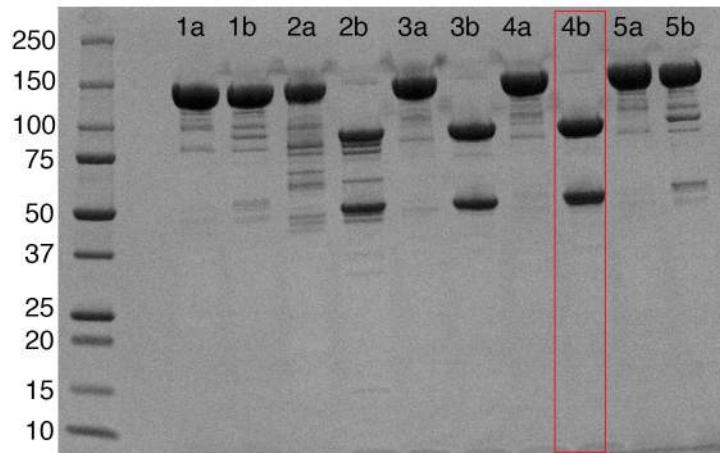
Fig. 3-1. The ideal trypsin to TeNT ratio to obtain activated toxin is 1:1000. Inactive TeNT was treated with varying concentrations of trypsin to determine the best enzyme/protein ratio. A protein molecular weight ladder is shown on the left. **1a**: no trypsin, no DTT, **1b**: no trypsin, w/DTT, **2a**: 1:10, no DTT, **2b**: 1:10 w/DTT, **3a**: 1:100, no DTT, **3b**: 1:100 w/DTT, **4a**: 1:1000, no DTT, **4b**: 1:1000 w/DTT, **5a**: 1:10,000, no DTT, **5b**: 1:10,000 w/DTT. Red box indicates good digestion of TeNT; the disulfide bond linking the heavy and light chains is reduced with DTT.

Specimen Preparation and EM

Uranyl formate (0.7% wt/vol) was used for conventional negative staining as previously described [197]. Images of un-nicked and nicked forms of TeNT were recorded using a Tecnai F20 electron microscope (FEI) equipped with a field emission electron source and operated at an acceleration voltage of 200kV. Images were taken under low-dose conditions at a magnification of 67,000X using a defocus value of -1.5 µm. Images were recorded on a Gatan 4K x 4K CCD camera. Images were converted to mixed raster content (mrc) format, and binned by a factor of 2, yielding final images with a 3.5 Å/pixel. Particle images of

the un-nicked and nicked forms of TeNT were selected using EMAN [219] and analyzed using SPIDER and the associated display program WEB [198].

Un-nicked TeNT and nicked TeNT Processing

Single particles of each toxin type were aligned and classified using the software Boxer [219] and Spider [220].

Crystal Structure Filtering

The crystal structures for BoNT/A (pdb: 3BTA, [146]) and BoNT/E (pdb:3FFZ, [148]) were selected for resolution-filtering. Their pdb coordinate files were converted into a mixed raster content (mrc) format using SPARX (single particle analysis for resolution extension) [221] with an Angstrom to pixel ratio of 3.5 and a box size of 72. The resulting density map was resolution-filtered to approximately 40 Å using EMAN2 [222] and was visualized using CHIMERA [199].

Results

The activation of TeNT does not induce an observable conformational change

Images were collected of both the inactive (un-nicked) form of TeNT and the active (nicked) form. A total of 5,133 inactive particles and 5,064 activated particles were selected for class averages. The un-nicked and nicked TeNT

particles were each sorted into fifteen class averages (Fig. 3-2a, 3-2b) using reference free alignment. The two forms of TeNT appeared to have similar structures. Both forms of the toxin adopted a "J" shape that could be grouped in three predominant orientations depending on their interaction with the grid surface. Four globular domains were observed within the "J" shaped molecules. Interestingly, no observable conformational changes between the un-nicked and nicked toxins could be detected at the EM level of resolution.
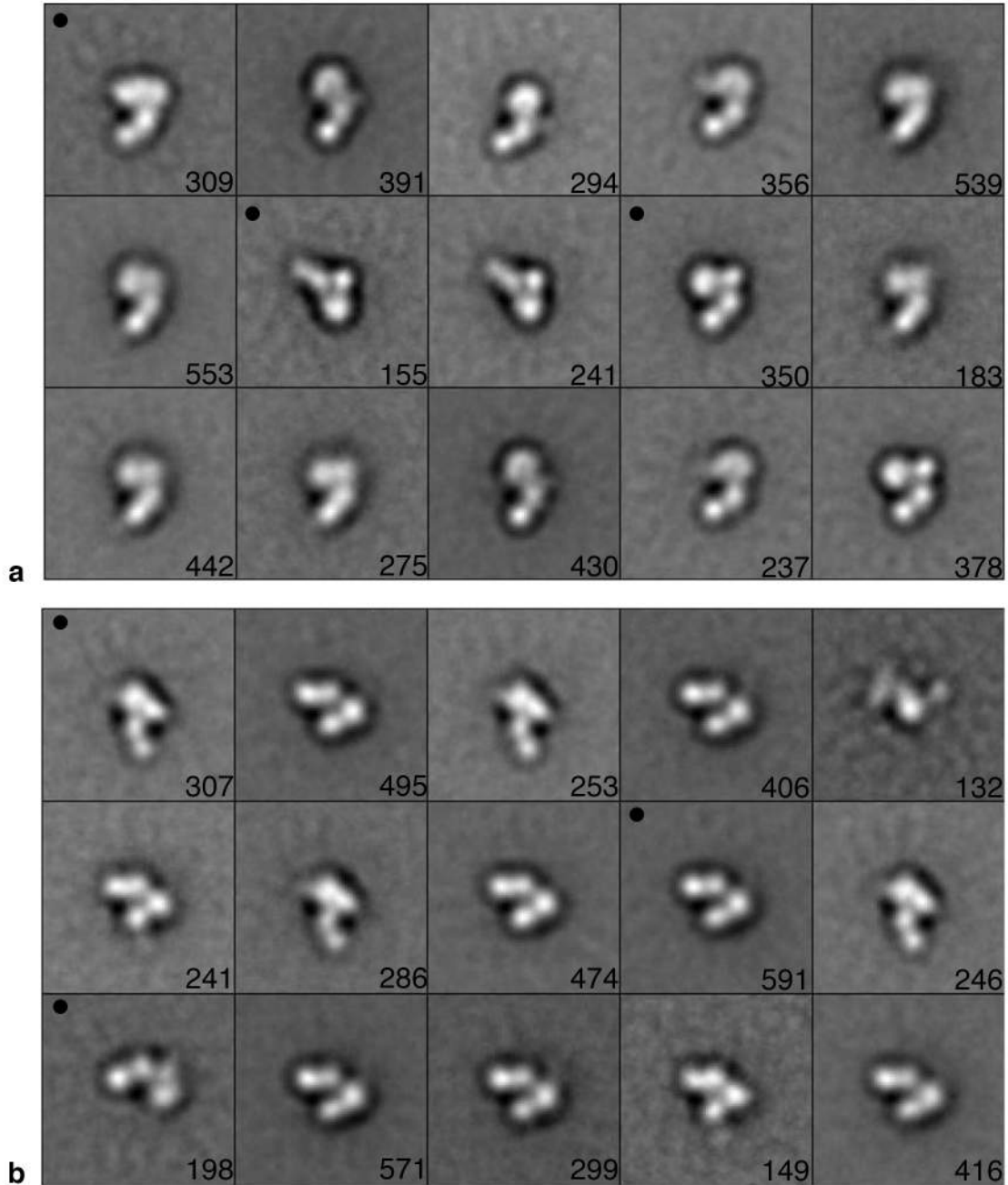
Fig. 3-2. Inactive TeNT and activated TeNT have similar structures by EM. (a) 5,133 un-nicked TeNT particles were aligned and sorted into 15 class averages. (b) 5,064 nicked TeNT particles were aligned and sorted into 15 class averages. There is no observable conformation change (by EM) between inactive and trypsin activated TeNT. The majority of class averages for both toxin types contain three variations of "J" shaped molecules with four globular domains visible. Side length of panels, 240 Å.

Reference–based alignments were performed to verify that there was no distinct conformation change between the two toxin types. Three representative classes were selected from the un-nicked and nicked toxins (Fig. 3-2a, 3-2b, black dots). The three un-nicked classes were used for referenced-based alignments against the entire population of nicked particles (Fig. 3-3a). Conversely, the three nicked classes were used against all of the un-nicked particles (Fig. 3-3a). Conformational differences between the two toxin types would, in theory, be more pronounced by aligning the entire population of one toxin type against three references representing the other toxin type. The un-nicked population of particles (Fig. 3-3b) and the nicked population (Fig. 3-3c) aligned reasonably well into either set of input references (3-3a). We observed that there were no significant differences in structure between the two populations of toxin particles, suggesting that the activation of TeNT does not induce a dramatic conformational change in the molecule. A higher resolution (crystal) structure of the holotoxin could reveal more subtle changes in the structure.
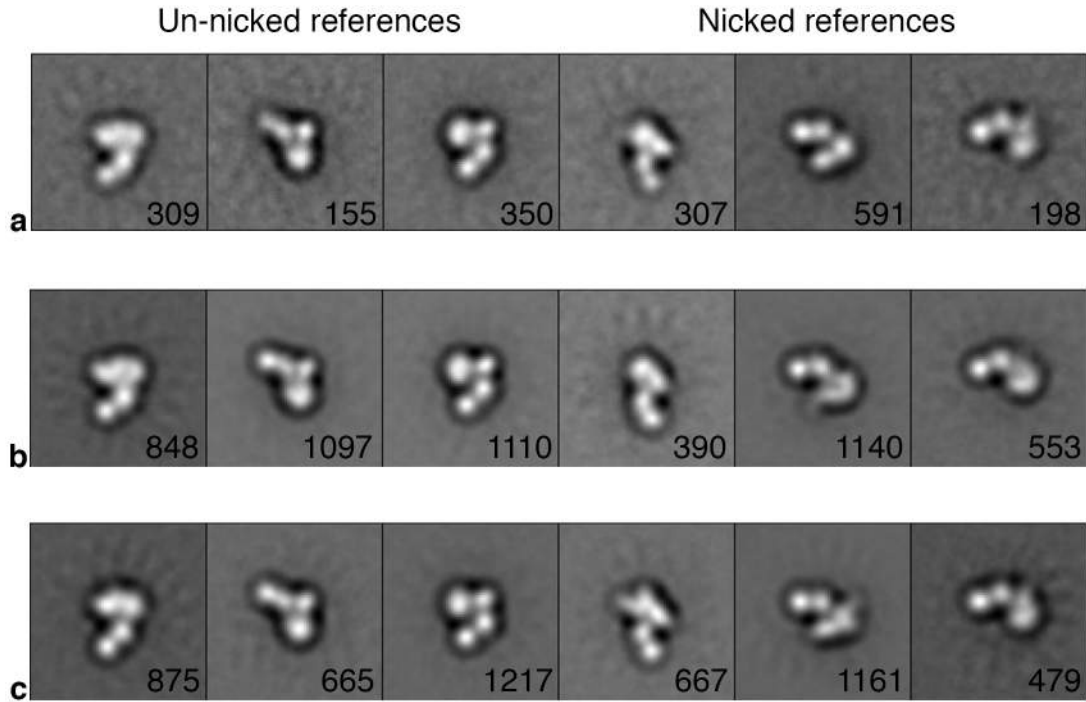
Fig. 3-3. Referenced-based alignments to compare the structures of the two forms of TeNT. (a) The three un-nicked input references are to the left while the three nicked references are to the right. (b) A reference-based alignment using the six references from (a) against 5,133 un-nicked particles. (c) A reference-based alignment using the six references from (a) against 5,064 nicked particles.

Negative stain EM averages of TeNT more closely resemble EM averages of BoNT/E than BoNT/A

The high resolution structure of BoNT/A [146] revealed the structural organization of its three domains. In it the binding and catalytic domains flank the translocation domain (Fig. 3-4a). Interestingly, the structure of BoNT/B [148] was also found to also have this "flanking" orientation for its domains (Fig. 3-4b). Before the crystal structure of BoNT/E was determined in 2009 [148] analysis of its structure had been investigated using negative stain EM and single particle averaging by Fischer *et al.* [223]. Work done by Fischer *et al.* used the structural

organization of type /A to guide their assessment of the type /E structure. Both toxins were negatively stained and sorted into class averages. The BoNT/A classes clearly illustrated the same organization as its crystal structure (Fig. 3-4a, Fig. 3-5a). The BoNT/E class averages provided the first insight that the /E toxin had a unique organization as compared to types /A and /B (Fig. 3-5b).

As stated earlier, the holotoxin structure for TeNT is unknown but crystal structures for its binding [149] (Fig. 3-4c) and catalytic [145](Fig. 3-4d) domains have been determined. These TeNT domains are very similar in structure to their known BoNT homologs.
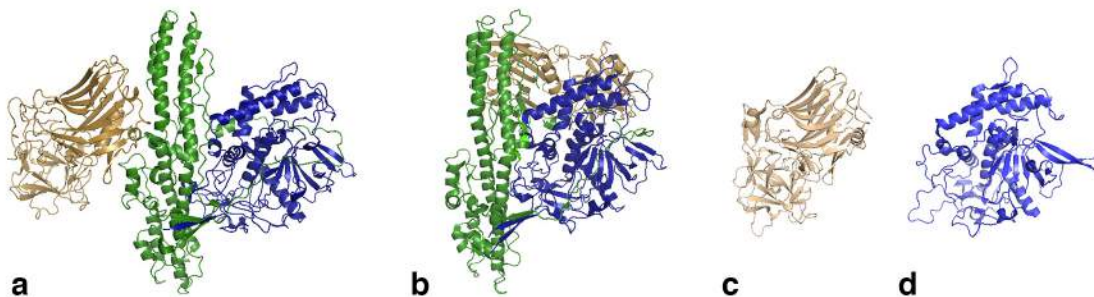
Fig. 3-4. Crystal structures for BoNT/A, BoNT/E, and two TeNT domains. For each toxin type the domains are colored: binding=beige, translocation=green, and catalytic=blue. (a) The translocation domain of BoNT/A is flanked by its binding and catalytic domains. (b) The BoNT/E structure has the binding and catalytic domains on one side of the translocation domain. (c) The TeNT binding and (d) catalytic domains have similar folds as their BoNT homologs.

We were interested to see if more structural insight of TeNT could be gained utilizing an EM approach similar to the one used for BoNT/E. We compared class averages of BoNT types /A and /E generated by Fischer *et al.* (Fig. 3-5a and b) to our classes of active form TeNT (Fig. 3-5c). The two

structural organizations of /A and /E are evident by negative stain. Our TeNT class averages did not appear to adopt an /A –like structure and more closely resembled that of type /E. We next filtered both the /A and /E crystal structures to ~40 Å and placed them in similar orientations as their representative class averages (Fig. 3-5d, e, and h). Both filtered structures were rotated over an array of angles. It was of interest to see if either the filtered /A or /E would generate a "J" shaped structure. The filtered /A structure formed some what of a "J" shaped structure when it was rotated to its side (Fig. 3-5g), but on an EM grid with negative stain this orientation would likely not be preferred. The /E filtered structure however could make J" shaped structures when rotated (Fig. 3-5f). The two TeNT domain crystal structures were aligned with the /E crystal structure in an attempt to predict how the domains of TeNT may be arranged (Fig. 3-5i). In this model the TeNT binding domain forms the "lower loop of the J" while the cross at the top of the "J" shape has the catalytic domain on the left and the translocation domain on the right. We hypothesize that the helices of the translocation domain are compressed behind the structure and interacting with the grid surface.
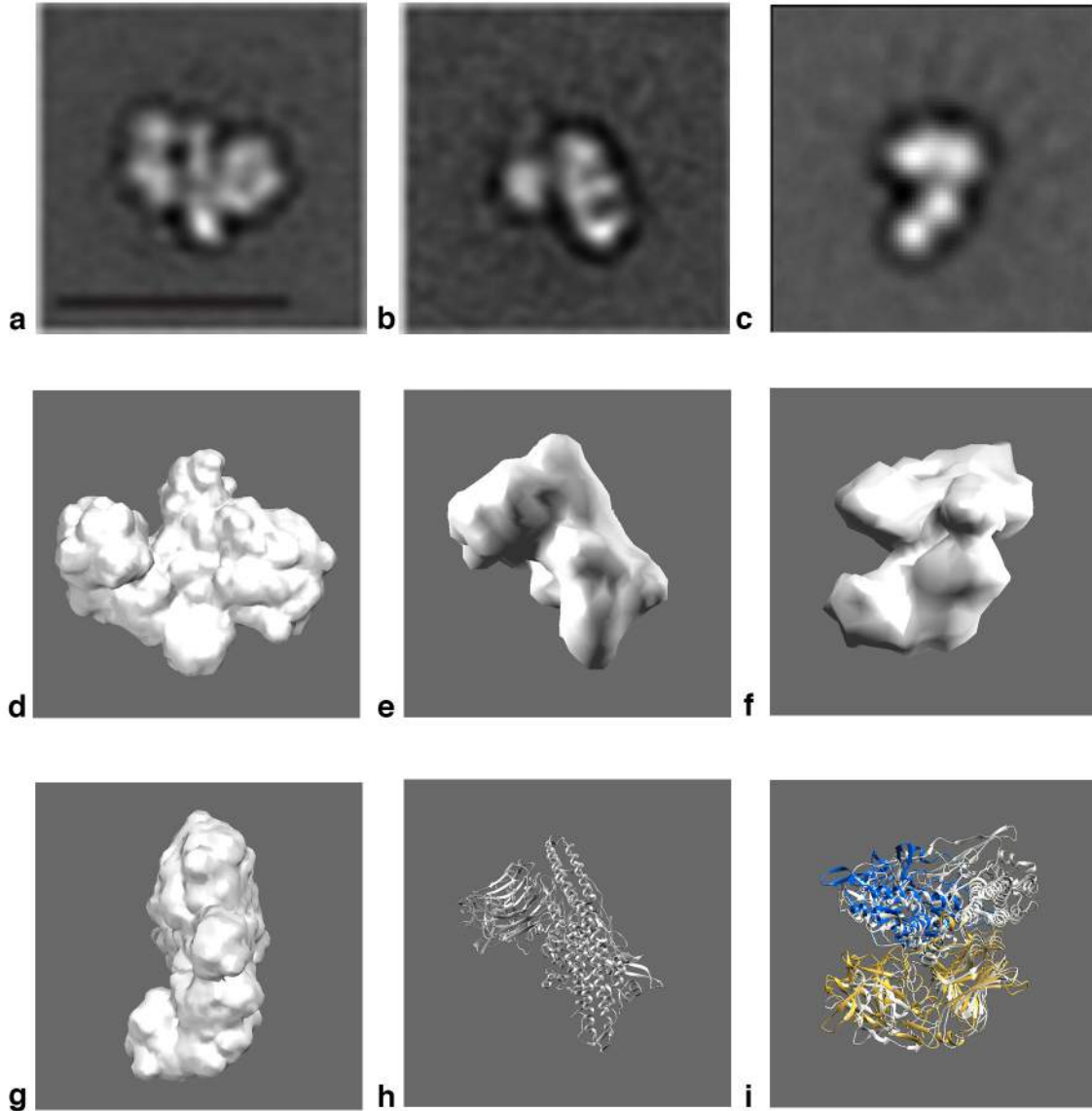
Fig. 3-5. TeNT resembles the organization of BoNT/E more than BoNT/A. (a) and (b) 2D class averages of BoNT/A and BoNT/E from Fischer *et al.* [223]. (c) 2D class average of nicked TeNT. (d) BoNT/A filtered to a resolution of ~ 40 A. (e) BoNT/E filtered to a resolution of ~ 40 A. (f) Filtered BoNT/E can be rotated to form the "J" shape observed in the TeNT 2D averages. (g) Filtered BoNT/A does not form a satisfactory "J" shape after rotation. (h) BoNT/E crystal structure in same orientation as (b) and (e). (i) TeNT catalytic domain (blue) and binding domain (gold) are aligned with BoNT/E structure seen in (f).

Discussion

Given the significant sequence homology between TeNT and the BoNTs it is not surprising that the structures of the two crystallized domains from TeNT so closely resemble their BoNT homologs. BoNT/E has a unique organization compared to the other serotypes (/A and /B) that cause human botulism. The significance of this structural difference in /E is still being explored. One hypothesis is that the consolidation of the domains to one side of the translocation domain may contribute to a faster release of the catalytic domain into the neuronal cytosol [224].

Here we present analysis of the TeNT holotoxin by negative stain EM and single particle averaging. We have observed that there is no discernable difference in toxin conformation after being activated with trypsin cleavage and that the TeNT molecules have a "J" shape. When our 2D averages of activated TeNT were compared to those of BoNT/A and /E we saw that of the two known BoNT structures TeNT was more closely related to /E. To explore this further, the two BoNT structures were filtered to approximately 40 A. These structures were each studied from an array of rotational angles in an effort to determine if either filtered structure could make a "J" shape. BoNT/A did not make a satisfactory "J" shape while the filtered /E molecule did. The structures of the two TeNT domains were aligned with their /E homologs and showed that TeNT likely has an organization more like /E.

To confirm this hypothesis, we propose to try some labeling techniques. Unfortunately, there are limited monoclonal antibodies for TeNT available commercially. Our recombinant TeNT construct is engineered with a N-terminal 6xHis tag, however, that could potentially be labeled with gold nanoparticles designed to interact with the His tag. An alternative approach to evaluate the structure would be to try generating a 3D reconstruction of TeNT using the random conical tilt approach [196]. This may be challenging to accomplish due the small size of the toxin. Lastly, and ideally, we would like to determine the high-resolution structure of TeNT. Crystallization trials are currently underway and will hopefully yield conclusive evidence that the TeNT holotoxin structure is similar to BoNT/E.

CHAPTER IV

CONCLUSIONS AND FUTURE DIRECTIONS

Conclusions

BoNT and TeNT and their associated diseases continue to sicken people around the world. The potential weaponization of BoNT and its use in an act of bioterrorism is considered a real threat to society. Remarkably, these toxins are also appreciated for their clinical applications to treat many dystonias of the musculature and for their unique mechanisms that researchers have used to better understand the function of the brain. Previous structural work on the CNTs has provided additional insight on the function of the toxins and has helped better explain their mechanisms for pathogenesis. In my thesis work, I have shown the molecular organization for the accessory proteins that interact with BoNT to form progenitor complexes and I have also determined low-resolution structures of the TeNT holotoxin

In Chapter II, I have presented 3D reconstructions of the three BoNT serotypes associated with human botulism using negative stain EM, single particle averaging, and the random conical tilt (RCT) method. Using these techniques I was able to successfully model the molecular organization for BoNT serotypes /A and /B. Both toxins were observed as ovoid shaped bodies that had an assembly of three arms with pincher shapes attached at a distal end. Using RCT, I was able to produce 3D density maps of the toxins and fit in crystal

structures of accessory proteins that are known to be a part of the complex. This was the first visualization of these complexes whose structure had been a matter of debate for quite some time. I noticed a large degree of flexibility in the /A complex, especially in the arm assembly at the end. I was able to explore this by producing movies made from many individual classes. These movies showed the degree of flexibility these complexes could have and helped us conceptualize how the structure could interact with the epithelial cells in the small intestine. BoNT/E was observed as an ovoid body, which was consistent with what was known about its accessory proteins. While I was unable to successfully use my 3D reconstruction to predict its molecular assembly it was still the first time the BoNT/E complex was visualized.

In Chapter III, I describe characterization of the EM the structure of the TeNT holotoxin. Two of the toxins three domains have had their structures determined but the overall architecture of all three domains is not known. Using negative stain EM and single particle averaging. I was able to produce novel images of the holotoxin. With this study, I demonstrated that inactive TeNT and TeNT activated by proteolytic cleavage were similar in structure, and no discernable conformational changes occurred as a result of TeNT nicking. I went on to compare my nicked TeNT 2D averages with those of BoNT/A and /E that were generated by another research group. These comparisons revealed that the TeNT holotoxin appears to resemble the /E structure rather than /A.

In total, these studies have provided novel visualizations of the two most potent toxins on the planet. By understanding the progenitor complex organization we have created a framework for understanding how the protein, BoNT, survives passage through the harsh conditions found in the intestinal tract and how the toxin design facilitates sampling and binding to the epithelial surface in the intestine. While the structural work on the TeNT holotoxin is still preliminary, I have been able to make some reasoned predictions of how its three domains are organized. Many structure related questions remain for both of the clostridial neurotoxins, some of which I have begun to address and will be discussed in the following section.

Preliminary Data for Future Directions

The HA3 – NTNH Interface

In Chapter II, I described our work on imaging BoNT PCs and detailing the molecular organization for serotypes /A and /B. I was unable to address, due to limitations in resolution, how the HA3 trimer interacted with the NTNH protein. In a structural sense, this protein interface is interesting because a symmetrical assembly of proteins (the HA3 trimer) is able to interact with an asymmetrical protein (NTNH). It is also interesting in a biomedical sense because this interaction likely contributes towards directing the toxin to the intestinal epithelial

cell layer. NTNH has a flexible loop at its end that is predicted to interact with the central pore of the HA3 trimer [225]. However, the residues involved in this interaction are not defined. In addition, it's unknown if there are additional residues on the surface of either protein surface that contribute to this interaction.

A better understanding of this protein interaction will provide new research possibilities in the engineering of HA3-NTNH like assemblies that could target other cell types or provide more insight into how this interaction helps direct the toxin to the epithelial cell layer. This could influence the design of future drugs or therapeutics that are able to localize to particular areas in the body and possibly direct their absorption.

Preliminary data

It has been well documented in the literature that the NTNH protein spontaneously nicks in its flexible loop region and that once this loop is nicked the protein can no longer interact with HA3 [225–229].

We synthesized the type /A NTNH gene and had it placed into a pET24-b expression vector with the restriction sites NdeI and XhoI. The protein has a 6xHis tag at the C-terminus and a predicted molecular weight of 139 kDa. Transformed BL-21 *E. coli* expressed the protein reasonably well though nicking of the protein was evident by Coomassie gel (Fig. 4-1).
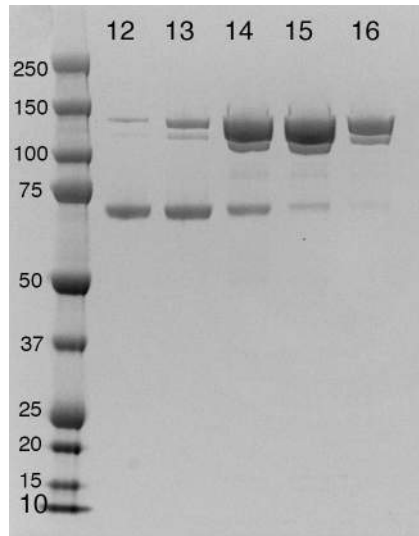
Fig. 4-1. Full-length NTNH sizing column fractions. The bands from fraction 13 were analyzed by Mass Spectrometry to confirm that the middle band was nicked NTNH. The lower band was from the *E. coli* protein ArnA.

Dr. Yukako Fujinaga, from Osaka University, provided us with a recombinant construct for type /A HA3. The HA3 gene was inserted into a pET52-b expression vector with the restriction sites KpnI and SalI. The protein has a N-terminal 6xHis tag and a C-terminal StrepTag II. An HA3 monomer has a predicted weight of ~70 kDa. This plasmid was transformed into BL-21 STAR *E. coli* cells for expression (Fig. 4-2).
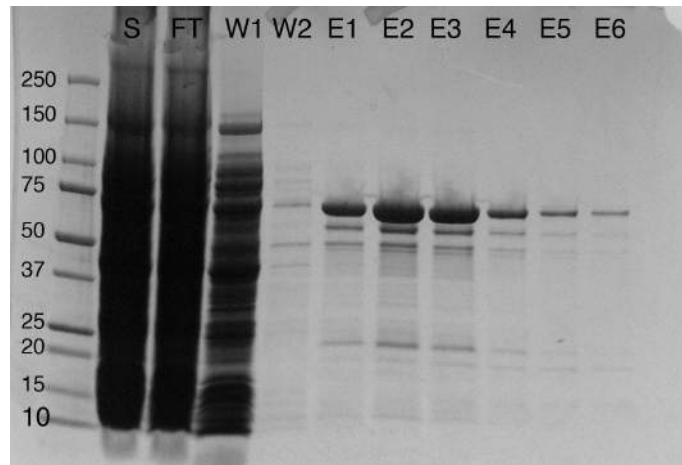
Fig. 4-2. HA3 fractions from Strep-Tactin resin. S: supernatant, FT: flow through, W1-2: 3 mL washes with binding buffer consisting of: 1.5 M NaCl, I M Tris-HCl, and 10 mM EDTA, pH 8.0. E1-6: 3 mL elution fractions with binding buffer and 2.5 mM desthiobiotin.

When the HA3 elution fractions were pooled and run over the sizing column, we observed that the protein tended to oligomerize into large assemblies but would also elute as the HA3 trimer (Fig. 4-3a). It was determined that the HA3 protein formed the larger assemblies as a result of concentration and that less concentrated protein over the column produced more trimeric HA3. Negative stain EM grids were prepared of the HA3 trimer (Fig. 4-3b).
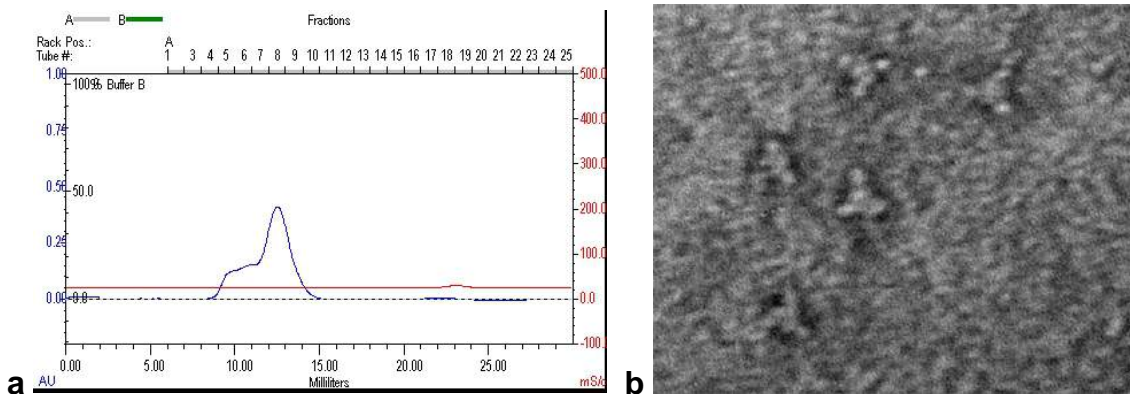
Fig. 4-3. HA3 purification. a) An FPLC trace of HA3 at pH 7.0. The short peak on the left corresponds to oligomers and the taller peak to the right corresponds to a HA3 trimer. b) A negative stain EM image of HA3 trimers.

We also engineered a truncated NTNH construct that consisted of the toxin's LC homolog (Fig. A-4a, the red domain). I refer to this construct as nLC (NTNH-LC). It is in a pET24-b expression vector with the restriction sites NheI and XhoI. The protein has a 6xHis tag at the C-terminus and a predicted molecular weight of ~50 kDa. This plasmid was transformed into BL-21 *E. coli* cells for expression (Fig. 4-4b).
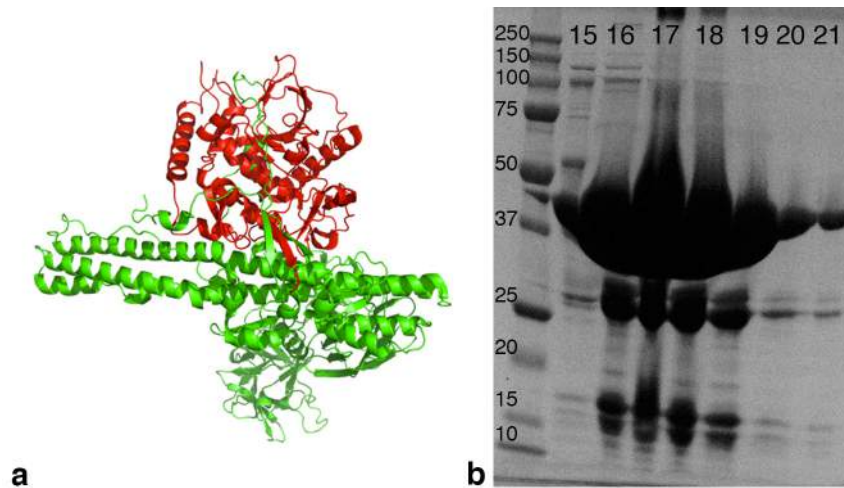
Fig. 4-4. The nLC construct. (a) The BoNT/A NTNH molecule is shown in green and its LC equivalent (nLC) is colored in red [225]. (b) Sizing column fractions.

I attempted to assess the binding of nLC and HA3 by gel filtration binding chromatography. Binding experiments were performed at 4° C on an analytical (Superdex 75) sizing column using two different buffer conditions: 50 mM Bis-Tris, pH 5, 100 mM NaCl *or* 50 mM Tris, pH 7.5, 100 mM NaCl. The pH 7.5 was used because a previous report using a synthesized nLC-loop only construct had been shown to interact with HA3 up to pH 7.6 [183]. The proteins were used in 1:1 picomolar concentrations for the binding assays. My intent with these assays was to establish the binding interaction between the two proteins. I planned to generate a series of HA3 point mutants to identify residues important for binding.

Any binding interaction at pH 5 could not be confirmed by Coomassie gel (Fig. 4-5a), or at pH 7.5 (Fig. 4-5b).
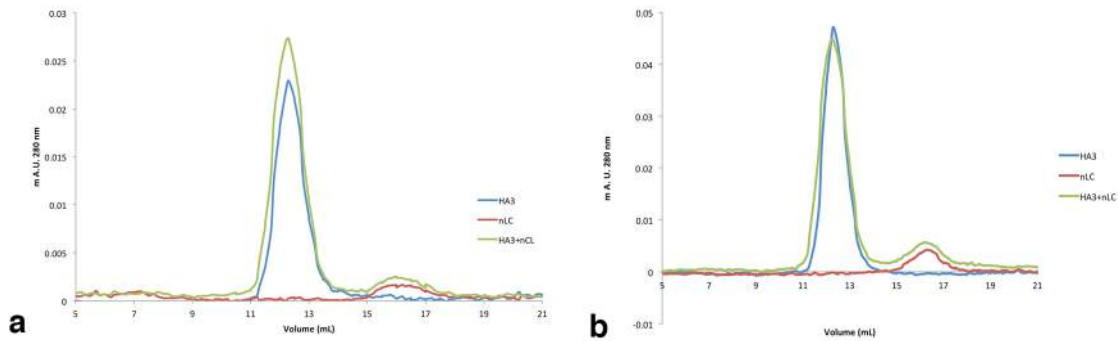
Fig. 4-5. nLC and HA3 gel filtration binding assays at pH 5 and pH 7.5. a) assay at pH 5.0. b) assay at pH 7.5. The small peaks on the left of each graph are unbound protein. This is likely due to the presence of nicked nLC in the protein sample.

I did not pursue the binding assays further because at the time I was having a difficult time generating enough HA3 (trimeric form) protein to try the assay at higher concentrations. I also felt that the presence of nicked nLC was a variable that could not be controlled and compromised the assay.

I did not have a chance to try co-crystallization trials with nLC and HA3, but I think this is worth pursuing.

BoNT/E Accessory Proteins

There is very little known about the additional genes in the BoNT/E gene locus: OrfX1, OrfX2, or p47. The Orf proteins are predicted to be accessory proteins to the neurotoxin but there is currently no evidence to support this claim. The purified BoNT/E PC we received from List Biologicals for our EM characterization did not include these proteins. With many thanks to Dr. Yukako

Fujinaga, we now have recombinant constructs for all three proteins. It would be interesting to pursue both structural and functional elements of these proteins as virtually nothing is known about them.

It would also be interesting to determine the high-resolution structure of the BoNT/E PC. This is comprised of two proteins: the neurotoxin and NTNH. As discussed earlier, the functional domains of the /A and /E neurotoxins are organized very differently from one another. The recent structure of BoNT/A and its NTNH showed that the proteins had the same structure and formed a protective complex by interlocking with one another. The RBD of BoNT/A underwent a large conformational shift when in complex with NTNH. Since The RBD and LC of type /E are positioned on the same side of the translocation domain, any conformational changes that occur from interacting with NTNH are hard to predict. In light of what's known about the BoNT/A-NTNH structure, many questions can be raised. Does the rearrangement of the binding domain influence the ability of the toxin to access its receptor or does it only act to protect the binding domain from proteolysis?

High-Resolution TeNT

I have also worked to crystallize the TeNT holotoxin and am encouraged by my preliminary results. It would be very interesting to have a high-resolution structure of the molecule to compare and contrast to its BoNT homologs. I am especially interested to know on an atomic level how TeNT may resemble BoNT/E and if it does, could it be engineered to interact with the type /E NTNH protein? Would this be sufficient to make TeNT orally toxic? Is there a structural difference between BoNT and TeNT that impacts how the toxin is sorted in the motor neuron?

Preliminary data on high-resolution TeNT

As mentioned earlier, the TeNT holotoxin structure is currently unknown. My negative stain analysis suggests that the structure is similar to BoNT/E. Additional EM work on TeNT should include domain assignment. This could be attempted with monoclonal antibody or gold nano-particles labeling. While doing my TeNT EM studies I also set out to crystallize the TeNT protein. The protein was purified as described in Chapter III Methods and was used for crystallization trials at a range of concentrations in un-nicked or nicked forms. The commercial broad screens Crystal Screen I & II, Index (from Hampton) and JCSG (from Qiagen) were used as well as our in-house Ben Screens (i-V) and John Screens (I and II).

One immediate observation I made was that the un-nicked TeNT was less soluble and quickly precipitated or "oiled out" in many of the screen conditions. The nicked form of the protein was more soluble in the screens and rarely "oiled out". I got promising crystal hits in Ben Screen II. These trays were set up nicked TeNT at 7 mg/mL. Crystals appeared after 12 days (Fig. 4-6).
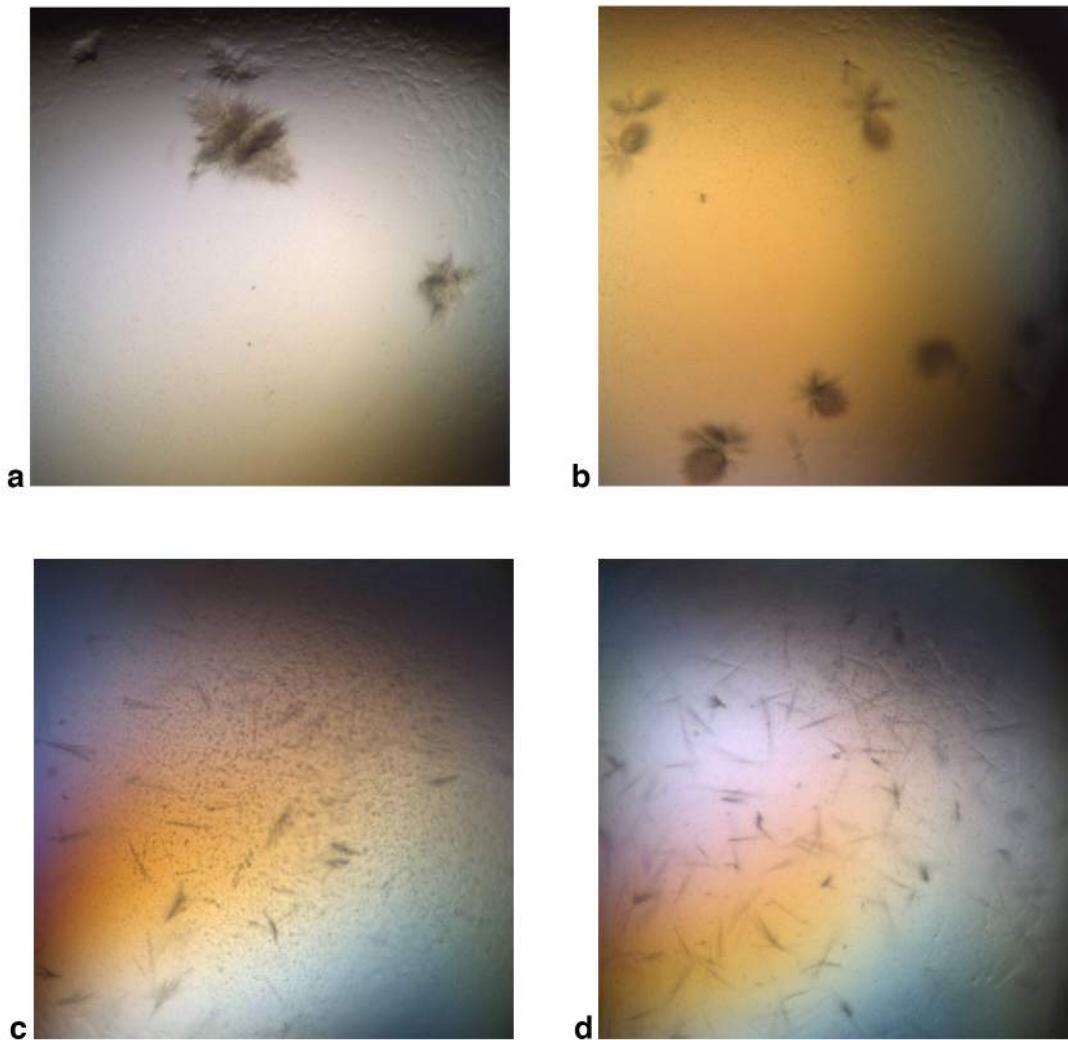
Fig. 4-6. Nicked TeNT at 7 mg/mL hits from Ben Screen II. (a) well A5, 100 mM Bis-Tris pH 5.0, 200 mM NaCl, 25% PEG 400 (b) well A6, 100 mM Bis-Tris pH 5.0, 200 mM NaCl, 30% PEG 400 (c) well E5, 100 mM Bis-Tris pH 5.0, 200 mM Ammonium Sulfate, 25% PEG 400 (d) well F5, 100 mM Bis-Tris pH 6.0, 200 mM Ammonium Sulfate, 25% PEG 400

I tried optimizing all of the hits shown above by varying the pH, salt concentration, and PEG 400 percentage. I got the best results using 100 mM Bis-Tris pH 6.0, a 25% - 30% range of PEG 400, and a 200 mM – 350 mM range of Ammonium Sulfate. 200 mM Ammonium Sulfate and 30% PEG 400 produced the best crystals. They were small single rods (Fig. 4-7) (approximately 25 um x 100 um). Some rods were harvested and sent to the Synchrotron. While a data set was not collected the crystals were protein and diffracted to ~8-9Å.

Attempts to generate larger crystals were unsuccessful. There is also the possibility the crystals were not TeNT and were a contaminant. For future attempts I recommend increasing the protein concentration and revisiting all of the broad crystallization screens. For any future optimization crystal trays I suggest varying the hanging drop sizes and the ratio between the protein and the mother liquor.

Fig. 4-7. Nicked TeNT at 8.5 mg/mL. 100 mM Bis-Tris pH 6.0, 200 mM Ammonium Sulfate, 30% PEG 400.

Additional Future Directions to Consider

In addition to the structure-based future directions discussed above there are many functional questions that remain regarding the CNTs. For example, the BoNT receptor on intestinal epithelial cells has yet to be defined. It is unknown if gangliosides, a protein receptor, or both are required for BoNT binding to the epithelial cell. Our lab possesses a siRNA (small interfering RNA) library screen that could be used towards this receptor identification.

BoNT oral toxicity is largely due to its ability to form PCs that protect it from degradation but research has also shown [182] that ingestion of large quantities of pure BoNT can be toxic. This suggests to me that TeNT can also be orally toxic if consumed in large enough quantities. If so, it would be of interest to use the siRNA screen to identify it's intestinal epithelial cell receptor. This also raises the question as to why *C. tetanii* spores in the intestinal tract do not result in tetanus cases in infants whereas infants are at risk of botulism if *C. botulinum* spores are ingested. Research in germ-free mice concluded that *C. tetanii* spores do not germinate in the intestine [230] but the reason for this remains unclear. Presumably, *C. tetanii* and *C. botulinum* spores require different environmental conditions for germination aside from an anaerobic habitat. The complete genome for *C. tetanii* and many *C. botuilnum* strains have been determined. Additionally, it is now known that *C. botulinum* has quorum sensing systems [231] and two-component systems (reviewed in [45]). I think it would be interesting see how the *C. tetanii* genome and *C. botulinum* genomes differ with regard to these signaling mechanisms.

It is also of interest to define the role of BoNT-PC HA proteins in absorption in the gastrointestinal tract. We are in possession of recombinant constructs for the three HA proteins that are part of the BoNT/A and /B PC (HA1, HA2, and HA3). It would be interesting to incorporate a fluorescent marker into each of theses proteins and visualize their interaction with columnar, intestinal

epithelial cells using confocal microscopy. Our siRNA screen could also be useful

for identifying key cellular components required for HA absorption.

APPENDIX

LIST OF PUBLICATIONS

Benefield, D.A., Dessain, S.K., Shine, N., Ohi, M.D., Lacy, D.B. "Molecular assembly of botulinum neurotoxin progenitor complexes", *Proc. Natl. Acad. Sci. U.S.A.,* **2013**, 110(14), 5630-5635.

Schmitt, J., Karalewitz, A., Benefield, D.A., Mushrush, D.J., Spiller, B.W., Barbieri, J.T., Lacy, D.B. "Structural analysis of botulinum neurotoxin type G receptor binding", *Biochem.*, **2010**, 49(25), 5200-5205.

BIBLIOGRAPHY

[1]   J. Diamond, Lethal gift of livestock, in: Guns, Germs, and Steel, W. W. Norton & Company, New York, 1997: pp. 195–215.

[2]   C. Mann, 1491, Random House, New York, 2005.

[3]   G. Fracastoro, Fracastor - La Syphilis (1530) - Le Mal Francais (Extrait du Livre De contagioibus, 1546), Adrien Delahayf, Paris, 1869.

[4]   T. Birch, ed., The History of the Royal Society of London, For Improving of Natural Knowledge, From Its First Rise. Vol. II., The Royal Society of London, London, 1756.

[5]   H. Gest, The discovery of microorganisms by Robert Hooke and Antoni van Leeuwenhoek, Fellows of The Royal Society, Notes Rec. R. Soc. 58 (2004) 187–201.

[6]   J. Lederberg, Infectious History, Science (80-.). 288 (2000) 287–293.

[7]   S. Kitasato, Über den Tetanusbacillus, Z. Hyg. 7 (1889).

[8]   E. Van Ermengem, A new anaerobic bacillus and its relation to botulism (English version), Rev. Infect. Dis. 1 (1979) 701–719.

[9]   G. Sanchez, A. Burridge, Decision making in head injury management in the Edwin Smith Papyrus, Neurosurg. Focus. 23 (2007) 1–9.

[10]   J. Pearce, Notes on tetanus (lockjaw)., J. Neurol. Neurosurg. Psychiatry. 60 (1996) 332–332.

[11]   M. Crumplin, P. Starling, A surgical artist at war: the paintings and sketches of Sir Charles Bell 1809-1815, 2005.

[12]   F. Erbguth, Historical notes on botulism, Clostridium botulinum, botulinum toxin, and the idea of the therapeutic use of the toxin., Mov. Disord. 19 Suppl 8 (2004) S2–6.

[13]   K. Foster, P. Hambleton, C. Shone, Discovery of neurotoxins, in: K. Foster, P. Hambleton, C. Shone (Eds.), Treat. from Toxins Ther. Potential Clostridial Neurotoxins, CRC Press, Boca Raton, FL, 2007: pp. 2–3.

[14]   F. Erbguth, M. Naumann, On the systematic descriptions of botulism and botulinum toxin by Justus Kerner (1786-1862), J. Hist. Neurosci. 9 (2000) 218–220.

[15]   P. Sheth, Toxins to drugs: The case of botulinum toxin, Curr. Sci. 95 (2008) 1009–1011.

[16]   A. Carle, G. Rattone, Studio Esperimentale sull'eziologia del tetano, Accad. Di Med. Di Torino Giomale Della. 32 (1884) 174–179.

[17]   R. Gunn, Botulism: from van Ermengem to the present. A comment., Rev. Infect. Dis. 1 (2014) 720–1.

[18]   M. Pitzurra, The History of Tetanus in Eighth International Conference on Tetanus., Pythagora Press, Rome-Milan, 1989.

[19]   E. Behring, S. Kitasato, The mechanism of immunity in animals to diptheria and tetanus, Dtsch. Medizinishe Wocheschrift. 16 (1890) 1113–1114.

[20]   P. Guilfoile, Tetanus, Chelsea House Publishers, New York, 2008.

[21]   G. Landmann, Uber die Ursache der Darmstader Bohnenvergiftung, Hyg Rundsau. 10 (1904) 449–452.

[22]   J. Leuchs, Beitrage zur Kenntnis des Toxins und Antitoxins des Bacillus Botulinus, Ztschr. Hyg. U. Infekt. 65 (1920) 55–84.

[23]   G. Burke, The occurrence of Bacillus botulinus in nature, J. Bacteriol. 4 (1919) 541–553.

[24]   I. Bengston, Studies on organisms concerned as causitive factors in botulism, Hyg. Lab. Bull. 136 (1924).

[25]   E. Stackebrandt, F. Rainey, Phylogenetic relationships., in: J. Rood, B. McClane, J. Songer, R. Titball (Eds.), Clostridia Mol. Biol. Pathog., Academic Press, Inc., London, 1997: pp. 3–19.

[26]   M. Salton, K. Kim, Structure, in: S. Baron (Ed.), Med. Microbiol., 4th ed., University of Texas Medical Branch at Galveston, Galveston, 1996.

[27]   L. Simpson, Botulinum neurotoxin and tetanus toxin, Academic Press, Inc., San Diego, 1989.

[28]   O. Rossetto, M. Scorzeto, A. Megighian, C. Montecucco, Tetanus neurotoxin., Toxicon. 66 (2013) 59–63.

[29] M. Peck, Biology and genomic analysis of Clostridium botulinum in: Advances in Microbial Physiology, Academic Press, Inc., London, 2009.

[30] G. Sakaguchi, Clostridium botulinum toxins, Pharmac. Ther. 19 (1983) 165–194.

[31] M. Popoff, P. Bouvet, Genetic characteristics of toxigenic Clostridia and toxin gene evolution, Toxicon. 75 (2013) 63–89.

[32] K. Hill, T. Smith, C. Helma, L. Ticknor, B. Foley, R. Svensson, et al., Genetic diversity among Botulinum Neurotoxin-producing clostridial strains., J. Bacteriol. 189 (2007) 818–32.

[33] M. Nevas, M. Lindström, S. Hielm, K. Johanna, M. Peck, H. Korkeala, et al., Diversity of Proteolytic Clostridium botulinum Strains , Determined by a Pulsed-Field Gel Electrophoresis Approach Diversity of Proteolytic Clostridium botulinum Strains , Determined by a Pulsed-Field Gel Electrophoresis Approach, Appl. Environ. Microbiol. 71 (2005) 1311–1317.

[34] M. Sebaihia, M. Peck, N. Minton, N. Thomson, M. Holden, W. Mitchell, et al., Genome sequence of a proteolytic (Group I) Clostridium botulinum strain Hall A and comparative analysis of the clostridial genomes, Genome Res. 17 (2007) 1082–1092.

[35] M. Popoff, Botulinum neurotoxins: more and more diverse and fascinating toxic proteins., J. Infect. Dis. 209 (2014) 168–9.

[36] M. Peck, S. Stringer, A. Carter, Clostridium botulinum in the post-genomic era., Food Microbiol. 28 (2011) 183–91.

[37] S. Stringer, A. Carter, M. Webb, E. Wachnicka, L. Crossman, M. Sebaihia, et al., Genomic and physiological variability within Group II (non-proteolytic) Clostridium botulinum., BMC Genomics. 14 (2013) 333.

[38] S. Raffestin, J. Marvaud, R. Cerrato, B. Dupuy, M. Popoff, Organization and regulation of the neurotoxin genes in Clostridium botulinum and Clostridium tetani., Anaerobe. 10 (2004) 93–100.

[39] H. Skarin, T. Håfström, J. Westerberg, B. Segerman, Clostridium botulinum group III: a group with dual identity shaped by plasmids, phages and mobile elements., BMC Genomics. 12 (2011) 185.

[40] N. Dover, J. Barash, K. Hill, G. Xie, S. Arnon, Molecular Characterization of a Novel Botulinum Neurotoxin Type H Gene., J. Infect. Dis. (2013) 1–11.

[41] D. Giménez, A. Ciccarelli, Clostridium botulinum type F in the soil of Argentina., Appl. Microbiol. 16 (1968) 732–4.

[42] J. Suen, C. Hatheway, A. Steigerwalt, D. Brenner, Genetic Confirmation of Identities of Neurotoxigenic Clostridium baratii and Clostridium butyricum Implicated as Agents of Infant Botulism, J. Clin. Microbiol. 26 (1988) 2191–2192.

[43] X. Meng, T. Karasawa, K. Zou, X. Kuang, X. Wang, C. Lu, et al., Characterization of a neurotoxigenic Clostridium butyricum strain isolated from the food implicated in an outbreak of food-borne type E botulism, J. Clin. Microbiol. 35 (1997) 2160–2162.

[44] J. Barash, S. Arnon, A Novel Strain of Clostridium botulinum That Produces Type B and Type H Botulinum Toxins., J. Infect. Dis. (2013) 1–9.

[45] C. Connan, C. Denève, C. Mazuet, M. Popoff, Regulation of toxin synthesis in Clostridium botulinum and Clostridium tetani., Toxicon. 75 (2013) 90–100.

[46] F. Chen, G. Kuziemko, R. Stevens, Biophysical characterization of the stability of the 150-kilodalton botulinum toxin, the nontoxic component, and the 900-kilodalton botulinum toxin complex species., Infect. Immun. 66 (1998) 2420–5.

[47] S. Gu, S. Rumpel, J. Zhou, J. Strotmeier, Botulinum neurotoxin is shielded by NTNHA in an interlocked complex, Science (80-.). 335 (2012) 977–981.

[48] H. Bruggemann, S. Baumer, W.F. Fricke, A. Wiezer, H. Liesegang, I. Decker, et al., The genome sequence of Clostridium tetani, the causative agent of tetanus disease., Proc. Natl. Acad. Sci. U. S. A. 100 (2003) 1316–21.

[49] J. Marvaud, M. Gibert, K. Inoue, Y. Fujinaga, K. Oguma, M. Popoff, botR/A is a positive regulator of botulinum neurotoxin and associated non-toxin protein genes in Clostridium botulinum A., Mol. Microbiol. 29 (1998) 1009–18.

[50] S. Raffestin, B. Dupuy, J. Marvaud, M. Popoff, BotR/A and TetR are alternative RNA polymerase sigma factors controlling the expression of the neurotoxin and associated protein genes in Clostridium botulinum type A and Clostridium tetani., Mol. Microbiol. 55 (2005) 235–49.

[51] T. Kubota, N. Yonekura, Y. Hariya, E. Isogai, H. Isogai, K. Amano, et al., Gene arrangement in the upstream region of Clostridium botulinum type E

and Clostridium butyricum BL6340 progenitor toxin genes is different from that of other types., FEMS Microbiol. Lett. 158 (1998) 215–21.

[52] C. Cox, C. Hardegree, R. Fornwald, Effect of tetanolysin on platelets and lysosomes., Infect. Immun. 9 (1974) 696–701.

[53] S. Billington, B. Jost, J. Songer, Thiol-activated cytolysins: structure, function and role in pathogenesis., FEMS Microbiol. Lett. 182 (2000) 197–205.

[54] C.L. Hatheway, Toxigenic clostridia., Clin. Microbiol. Rev. 3 (1990) 66–98.

[55] R. V Considine, L.L. Simpson, Cellular and molecular actions of binary toxins possessing ADP-ribosyltransferase activity, Toxicon. 29 (1991) 913–936.

[56] D.M. Gill, Bacterial toxins: a table of lethal amounts., Microbiol. Rev. 46 (1982) 86–94.

[57] H. Bigalke, T. Binz, Mechanisms of Actions of Neurotoxins, in: K. Foster, P. Hambleton, C. Shone (Eds.), Treat. from Toxins Ther. Potential Clostridial Neurotoxins, CRC Press, Boca Raton, 2007: pp. 47–65.

[58] S. van Heyningen, Tetanus toxin, Phamacology Ther. 11 (1980) 141–157.

[59] I. Ohishi, Oral toxicities of Clostridium botulinum type A and B toxins from different strains., Infect. Immun. 43 (1984) 487–90.

[60] L. Cheng, T. Henderson, Comparison of oral toxicological properties of botulinum neurotoxin serotypes A and B., Toxicon. 58 (2011) 62–7.

[61] A. Maksymowych, M. Reinhard, C.J. Malizio, M.C. Goodnough, E. a Johnson, L.L. Simpson, Pure botulinum neurotoxin is absorbed from the stomach and small intestine and produces peripheral neuromuscular blockade., Infect. Immun. 67 (1999) 4708–12.

[62] I. Ohishi, S. Sugii, G. Sakaguchi, Oral toxicities of Clostridium botulinum toxins in response to molecular size., Infect. Immun. 16 (1977) 107–9.

[63] G. Sakaguchi, S. Sakaguchi, Oral toxicities of Clostridium botulinum type E toxins of different forms, Japanese J. Med. Sci. Biol. 27 (1974) 241–244.

[64] F. Chen, G. Kuziemko, R. Stevens, Biophysical characterization of the stability of the 150-kilodalton botulinum toxin, the nontoxic component, and

the 900-kilodalton botulinum toxin complex species., Infect. Immun. 66 (1998) 2420–2425.

[65] J. Mellanby, How does tetanus toxin work?, Neuroscience. 6 (1981) 281–300.

[66] T. Cook, R. Protheroe, J. Handel, Tetanus: a review of the literature., Br. J. Anaesth. 87 (2001) 477–87.

[67] W. Atkinson, C. Wolfe, J. Hamborsky, eds., Tetanus in: Epidemiology and Prevention of Vaccine-Preventable Diseases, 12th ed., Public Health Foundation, Washington, D.C., 2012.

[68] J. Sobel, Botulism, Clin. Infect. Dis. 41 (2005) 1167–1173.

[69] M. Cherington, Botulism: update and review., Semin. Neurol. 24 (2004) 155–63.

[70] D. Ciccarone, Heroin in brown, black and white: Structural factors and medical consequences in the US heroin market, Int. J. Drug Policy. 20 (2009) 277–282.

[71] H. Sugiyama, Studies on factors affecting the heat resistance of spores of Clostridium botulinum, J. Bacteriol. 62 (1951) 81–96.

[72] M. Peleg, M. Cole, Estimating the survival of Clostridium botulinum spores during heat treatments, J. Food Prot. 2 (2000) 155–291.

[73] L. Simpson, Identification of the characteristics that underlie botulinum toxin potency: implications for designing novel drugs., Biochimie. 82 (2000) 943–53.

[74] L. Fenicia, G. Franciosa, M. Pourshaban, P. Aureli, Intestinal toxemia botulism in two young people, caused by Clostridium butyricum type E., Clin. Infect. Dis. 29 (1999) 1381–7.

[75] L.M. McCroskey, C.L. Hatheway, Laboratory findings in four cases of adult botulism suggest colonization of the intestinal tract., J. Clin. Microbiol. 26 (1988) 1052–4.

[76] M. Brett, J. McLauchlin, A. Harris, S. O'Brien, N. Black, R. Forsyth, et al., A case of infant botulism with a possible link to infant formula milk powder: evidence for the presence of more than one strain of Clostridium botulinum in clinical specimens and food., J. Med. Microbiol. 54 (2005) 769–76.

[77] J. Park, L. Simpson, Inhalational Poisoning by Botulinum Toxin and Inhalation Vaccination with Its Heavy-Chain Component, Infect. Immun. 71 (2003) 1147–1154.

[78] A. Bakheit, C. Ward, D. McLellan, Generalised botulism-like syndrome after intramuscular injections of botulinum toxin type A: a report of two cases., J. Neurol. Neurosurg. Psychiatry. 62 (1997) 198–198.

[79] D. Chertow, E. Tan, S. Maslanka, J. Schulte, E. Bresnitz, R. Weisman, et al., Botulism in 4 adults following cosmetic injections with an unlicensed, highly concentrated botulinum preparation., JAMA. 296 (2006) 2476–9.

[80] C. Gilles, The isolation of tetnus bacilli from street dust, J. Am. Med. Assoc. 109 (1937) 484–486.

[81] T. Byrd, H. Ley, Clostridium tetani in a Metropolitan Area: A Limited Survey Incorporating a Simplified in Vitro Identification Test., Appl. Microbiol. 14 (1966) 993–7.

[82] H.H. Huss, Distribution of Clostridium botulinum, Appl. Environ. Microbiol. 39 (1980) 764–769.

[83] J. Brust, R. Richter, Tetanus in the inner city, N. Y. State J. Med. 74 (1974) 1735–42.

[84] I. Oladiran, D. Meier, A. Ojelade, D. OlaOlorun, A. Adeniran, J. Tarpley, Tetanus: continuing problem in the developing world., World J. Surg. 26 (2002) 1282–5.

[85] V. Dowell, Botulism and tetanus: selected epidemiologic and microbiologic aspects., Rev. Infect. Dis. 6 Suppl 1 (2014) S202–7.

[86] A. Sheth, P. Wiersma, D. Atrubin, V. Dubey, D. Zink, G. Skinner, et al., International outbreak of severe botulism with prolonged toxemia caused by commercial carrot juice., Clin. Infect. Dis. 47 (2008) 1245–51.

[87] J. Townes, P. Cieslak, C. Hatheway, H. Solomom, J. Holloway, M. Baker, et al., An Outbreak of Type A Botulism Associated with a Commercial Cheese Sauce, Ann. Intern. Med. 125 (1996) 558–563.

[88] J. Gray, Fonterra botulism crisis was false alarm, New Zeal. Her. (2013).

[89] S. Henson, B. Traill, The demand for food safety: Market imperfections and the role of government, Food Policy. 18 (1193) 152–162.

103

[90] P. Gronski, F.R. Seiler, H.G. Schwick, Discovery of antitoxins and development of antibody preparations for clinical uses from 1890 to 1990., Mol. Immunol. 28 (1991) 1321–32.

[91] P. Descombey, L'anatoxine tetanique, Comptes Rendus Hebomadaires Des Seances Mem. La Soc. Biol. 91 (1924) 223–234.

[92] G. Ramon, C. Zoller, De la valeur antigenique de l'antitoxine tetanique chez l'homme, Comptes Rendus Hebomadaires Des Seances l'Academie Des Sci. 182 (1926) 245–247.

[93] R. Raghuvanshi, Y. Katare, K. Lalwani, M. Ali, O. Singh, A. Panda, Improved immune response from biodegradable polymer particles entrapping tetanus toxoid by use of different immunization protocol and adjuvants, Int. Kournal Pharm. 245 (2001) 109–121.

[94] M. Weinberg, P. Goy, Recherches sur la toxine botulinque, Comptes Rendus Hebomadaires Des Seances Mem. La Soc. Biol. 90 (1924) 269–271.

[95] I. Velikanov, Immunization experimentale de l'homme contra la botulisme, Giorn. Batter. E Immunol. 17 (1936) 451.

[96] H. Reams, Studies on botulinum toxoid, types A and B, J. Immunol. 55 (1947) 309.

[97] P. Katona, Botulinum toxin: therapeutic agent to cosmetic enhancement to lethal biothreat., Anaerobe. 18 (2012) 240–3.

[98] S.S. Long, Infant Botulism and Treatment With BIG-IV (BabyBIG), Pediatr. Infect. Dis. J. 26 (2007) 261–262.

[99] S. Long, Infant botulism, Pediatr. Infect. Dis. J. 20 (2001) 707–710.

[100] F. Frischknecht, The history of biological warfare, EMBO Rep. 4 (2003) 47–52.

[101] S. Rumyantsev, The best defence against bioweapons has already been invented by evolution., Infect. Genet. Evol. 4 (2004) 159–66.

[102] A. Moscrop, Mass hysteria is seen as main threat from bioweapons, Br. Med. J. 323 (2001) 1023.

[103] L. Rotz, A. Khan, S. Lillibridge, S. Ostroff, J. Hughes, Public health assessment of potential biological terrorism agents., Emerg. Infect. Dis. 8 (2002) 225–30.

[104] S. Arnon, R. Schechter, T. Inglesby, D. Henderson, J. Bartlett, M. Ascher, et al., Botulinum toxin as a biological weapon: medical and public health management., JAMA. 285 (2001) 1059–70.

[105] J.C. Larsen, U.S. Army Botulinum Neurotoxin (BoNT) Medical Therapeutics Research Program: past accomplishments and future directions, Drug Dev. Res. 70 (2009) 266–278.

[106] CDC Select Agent Program, Atlanta, 2011.

[107] J. Jankovic, Botulinum toxin in clinical practice, J. Neurol. Neurosurg. Psychiatry. 75 (2004) 951–957.

[108] C. Montecucco, J. Molgó, Botulinal neurotoxins: revival of an old killer., Curr. Opin. Pharmacol. 5 (2005) 274–9.

[109] S. Ando, Gangliosides in the nervous system., Neurochem. Int. 5 (1984) 507–537.

[110] S. Hakomori, Glycosphingolipids in cellular interaction, differentiation, and oncogenesis., Annu. Rev. Biochem. 50 (1981) 733–764.

[111] M. Benson, Z. Fu, J.-J. Kim, M. Baldwin, Unique ganglioside recognition strategies for clostridial neurotoxins., J. Biol. Chem. 286 (2011) 34015–22.

[112] P. Emsley, The Structures of the HC Fragment of Tetanus Toxin with Carbohydrate Subunit Complexes Provide Insight into Ganglioside Binding, J. Biol. Chem. 275 (2000) 8889–8894.

[113] A.R. Kroken, A.P. Karalewitz, Z. Fu, M.R. Baldwin, J.-J.P. Kim, J.T. Barbieri, Unique ganglioside binding by botulinum neurotoxins C and D-SA., FEBS J. 278 (2011) 4486–96.

[114] B. Yowler, C.-L. Schengrund, Glycosphingolipids-sweets for botulinum neurotoxin., Glycoconj. J. 21 (2004) 287–93.

[115] T. Binz, A. Rummel, Cell entry strategy of clostridial neurotoxins., J. Neurochem. 109 (2009) 1584–95.

[116] K. Bercsenyi, F. Giribaldi, G. Schiavo, The elusive compass of clostridial neurotoxins: Deciding when and where to go?, Curr. Top. Microbiol. Immunol. 364 (2013) 91–113.

[117] M. Dong, F. Yeh, W. Tepp, C. Dean, E. Johnson, R. Janz, et al., SV2 is the protein receptor for botulinum neurotoxin A., Science (80-.). 312 (2006) 592–6.

[118] A. Nishikawa, N. Uotsu, H. Arimitsu, J.-C. Lee, Y. Miura, Y. Fujinaga, et al., The receptor and transporter for internalization of Clostridium botulinum type C progenitor toxin into HT-29 cells., Biochem. Biophys. Res. Commun. 319 (2004) 327–33.

[119] A. Rummel, T. Karnath, T. Henke, H. Bigalke, T. Binz, Synaptotagmins I and II act as nerve cell receptors for botulinum neurotoxin G., J. Biol. Chem. 279 (2004) 30865–70.

[120] J. Schmitt, A. Karalewitz, D. Benefield, D. Mushrush, R. Pruitt, B.W. Spiller, et al., Structural analysis of botulinum neurotoxin type G receptor binding ., Biochemistry. 49 (2010) 5200–5.

[121] R. Jin, A. Rummel, T. Binz, A.T. Brunger, Botulinum neurotoxin B recognizes its protein receptor with high affinity and specificity., Nature. 444 (2006) 1092–5.

[122] C. Montecucco, G. Schiavo, Structure and function of tetanus and botulinum, Q. Rev. Biophys. 28 (1995) 423–472.

[123] A. Rummel, T. Eichner, T. Weil, T. Karnath, A. Gutcaits, S. Mahrhold, et al., Identification of the protein receptor binding site of botulinum neurotoxins B and G proves the double-receptor concept., Proc. Natl. Acad. Sci. U. S. A. 104 (2007) 359–64.

[124] F. Yeh, M. Dong, J. Yao, W. Tepp, G. Lin, E. Johnson, et al., SV2 mediates entry of tetanus neurotoxin into central neurons., PLoS Pathog. 6 (2010) e1001207.

[125] C. Chen, M. Baldwin, J. Barbieri, Molecular basis for tetanus toxin coreceptor interactions., Biochemistry. 47 (2008) 7179–86.

[126] C.B. Harper, S. Martin, T.H. Nguyen, S.J. Daniels, N. a Lavidis, M.R. Popoff, et al., Dynamin inhibition blocks botulinum neurotoxin type A endocytosis in neurons and delays botulism., J. Biol. Chem. 286 (2011) 35966–76.

[127] S. Pust, H. Barth, K. Sandvig, Clostridium botulinum C2 toxin is internalized by clathrin- and Rho-dependent mechanisms., Cell. Microbiol. 12 (2010) 1809–20.

[128] K. Deinhardt, O. Berninghausen, H. Willison, C. Hopkins, G. Schiavo, Tetanus toxin is internalized by a sequential clathrin-dependent mechanism initiated within lipid microdomains and independent of epsin1., J. Cell Biol. 174 (2006) 459–71.

[129] G. Lalli, S. Bohnert, K. Deinhardt, C. Verastegui, G. Schiavo, The journey of tetanus and botulinum neurotoxins in neurons, Trends Microbiol. 11 (2003) 431–437.

[130] M. Montal, Botulinum neurotoxin: a marvel of protein design., Annu. Rev. Biochem. 79 (2010) 591–617.

[131] G. Lalli, S. Gschmeissner, G. Schiavo, Myosin Va and microtubule-based motors are required for fast axonal retrograde transport of tetanus toxin in motor neurons., J. Cell Sci. 116 (2003) 4639–50.

[132] M. Schwab, K. Suda, H. Thoenen, Selective retrograde transsynaptic transfer of a protein, tetanus toxin, subsequent to its retrograde axonal transport., J. Cell Biol. 82 (1979) 798–810.

[133] S. Bohnert, G. Schiavo, Tetanus toxin is transported in a novel neuronal compartment characterized by a specialized pH regulation., J. Biol. Chem. 280 (2005) 42336–44.

[134] R. Jahn, R.H. Scheller, SNAREs--engines for membrane fusion., Nat. Rev. Mol. Cell Biol. 7 (2006) 631–43.

[135] B. Poulain, M. Popoff, A. Fessard, How do the Botulinum Neurotoxins block neurotransmitter release: from botulism to the molecular mechanism of action, The Botulinum Journalnum. 1 (2008) 14–87.

[136] O. Rossetto, F. Deloye, B. Poulain, R. Pellizzari, G. Schiavo, C. Montecucco, The metallo-proteinase activity of tetanus and botulism neurotoxins., J. Physiol. Paris. 89 (1995) 43–50.

[137] C. Montecucco, How do tetanus and botulinum neurotoxins bind to neuronal membranes?, Trends Biochem. Sci. 11 (1986) 314–317.

[138] C. Montecucco, G. Schiavo, S. Biomediche, U. Padova, Mechanism of action of tetanus and botulinum neurotoxins, Mol. Microbiol. 13 (1994) 1–8.

[139] A.E. Polley, J. Vick, H. Ciuchta, D. Fischetti, F. Macchitelli, N. Montanarelli, Botulinum Toxin , Type A: Effects on Central Nervous System, Science (80-.). 147 (1965) 1036–1037.

[140] H. Wiegand, G. Erdmann, H. Wellhoner, 125I-Labelled Botulinum A Neurotoxin: Pharmacokinetics in cats after intramuscular injection, Naunyn. Schmiedebergs. Arch. Pharmacol. 292 (1976) 161–165.

[141] F. Antonucci, C. Rossi, L. Gianfranceschi, O. Rossetto, M. Caleo, Long-distance retrograde effects of botulinum neurotoxin A., J. Neurosci. 28 (2008) 3689–96.

[142] L. Restani, F. Giribaldi, M. Manich, K. Bercsenyi, G. Menendez, O. Rossetto, et al., Botulinum neurotoxins A and E undergo retrograde axonal transport in primary motor neurons., PLoS Pathog. 8 (2012) e1003087.

[143] Y. Humeau, F. Doussau, N.J. Grant, B. Poulain, How botulinum and tetanus neurotoxins block neurotransmitter release., Biochimie. 82 (2000) 427–46.

[144] G. Schiavo, O. Rossetto, F. Benfenati, B. Poulain, C. Montecucco, Tetanus and botulinum neurotoxins are zinc proteases specific for components of the neurocytosis apparatus, Ann. New York Acad. Sci. 710 (1994) 65–75.

[145] M. Breidenbach, A. Brunger, 2.3 A crystal structure of tetanus neurotoxin light chain., Biochemistry. 44 (2005) 7450–7.

[146] D.B. Lacy, W. Tepp, a C. Cohen, B.R. DasGupta, R.C. Stevens, Crystal structure of botulinum neurotoxin type A and implications for toxicity., Nat. Struct. Biol. 5 (1998) 898–902.

[147] S. Swaminathan, S. Eswaramoorthy, Structural analysis of the catalytic and binding sites of Clostridium botulinum neurotoxin B., Nat. Struct. Biol. 7 (2000) 693–9.

[148] D. Kumaran, S. Eswaramoorthy, W. Furey, J. Navaza, M. Sax, S. Swaminathan, Domain organization in Clostridium botulinum neurotoxin type E is unique: its implication in faster translocation., J. Mol. Biol. 386 (2009) 233–45.

[149] T. Umland, L. Wingert, Structure of the receptor binding fragment Hc of tetanus neurotoxin, Nat. Struct. Biol. 4 (1997) 788–792.

[150] A. Fischer, M. Montal, Molecular dissection of botulinum neurotoxin reveals interdomain chaperone function., Toxicon. 75 (2013) 101–7.

[151] C. Fotinou, P. Emsley, I. Black, H. Ando, H. Ishida, M. Kiso, et al., The crystal structure of tetanus toxin Hc fragment complexed with a synthetic GT1b analogue suggests cross-linking between ganglioside receptors and the toxin., J. Biol. Chem. 276 (2001) 32274–81.

[152] H. Louch, E.S. Buczko, M. Woody, R.M. Venable, W.F. Vann, Identification of a binding site for ganglioside on the receptor binding domain of tetanus toxin., Biochemistry. 41 (2002) 13644–52.

[153] D.B. Lacy, R.C. Stevens, Sequence homology and structural analysis of the clostridial neurotoxins., J. Mol. Biol. 291 (1999) 1091–104.

[154] M. Dong, D. Richards, M. Goodnough, W. Tepp, E. Johnson, E. Chapman, Synaptotagmins I and II mediate entry of botulinum neurotoxin B into cells., J. Cell Biol. 162 (2003) 1293–303.

[155] Q. Chai, J. Arndt, M. Dong, W. Tepp, E. Johnson, E. Chapman, et al., Structural basis of cell surface receptor recognition by botulinum neurotoxin B., Nature. 444 (2006) 1096–100.

[156] D.B. Lacy, R.C. Stevens, Sequence homology and structural analysis of the clostridial neurotoxins., J. Mol. Biol. 291 (1999) 1091–104.

[157] A. Fischer, M. Montal, Crucial role of the disulfide bridge between botulinum neurotoxin light and heavy chains in protease translocation across membranes., J. Biol. Chem. 282 (2007) 29604–11.

[158] A. Fischer, M. Montal, Single molecule detection of intermediates during botulinum neurotoxin translocation across membranes., Proc. Natl. Acad. Sci. U. S. A. 104 (2007) 10447–52.

[159] A. Fischer, D. Mushrush, D. Lacy, M. Montal, Botulinum neurotoxin devoid of receptor binding domain translocates active protease., PLoS Pathog. 4 (2008) e1000245.

[160] S. Sun, S. Suresh, H. Liu, W. Tepp, E. Johnson, J. Edwardson, et al., Receptor binding enables botulinum neurotoxin B to sense low pH for translocation channel assembly., Cell Host Microbe. 10 (2011) 237–47.

[161] M. Galloux, H. Vitrac, C. Montagner, S. Raffestin, M.R. Popoff, A. Chenal, et al., Membrane Interaction of botulinum neurotoxin A translocation (T) domain. The belt region is a regulatory loop for membrane interaction., J. Biol. Chem. 283 (2008) 27668–76.

[162] M. Pirazzini, O. Rossetto, P. Bolognese, C.C. Shone, C. Montecucco, Double anchorage to the membrane and intact inter-chain disulfide bond are required for the low pH induced entry of tetanus and botulinum neurotoxins into neurons., Cell. Microbiol. 13 (2011) 1731–43.

[163] L. Koriazova, M. Montal, Translocation of botulinum neurotoxin light chain protease through the heavy chain channel., Nat. Struct. Biol. 10 (2003) 13–8.

[164] A. Fischer, M. Montal, Crucial role of the disulfide bridge between botulinum neurotoxin light and heavy chains in protease translocation across membranes., J. Biol. Chem. 282 (2007) 29604–11.

[165] S. Swaminathan, Molecular structures and functional relationships in clostridial neurotoxins., FEBS J. 278 (2011) 4467–85.

[166] G. Schiavo, M. Matteoli, C. Montecucco, Neurotoxins affecting neuroexocytosis., Physiol. Rev. 80 (2000) 717–66.

[167] L.L. Pellegrini, V. O'Connor, F. Lottspeich, H. Betz, Clostridial neurotoxins compromise the stability of a low energy SNARE complex mediating NSF activation of synaptic vesicle fusion., EMBO J. 14 (1995) 4705–13.

[168] R. Pellizzari, O. Rossetto, S. Giovedi, E. Johnson, C. Shone, C. Montecucco, et al., Structural Determinants of the Specificity for Synaptic Vesicle-associated Membrane Protein / Synaptobrevin of Tetanus and Botulinum Type B and G Neurotoxins, J. Biol. Chem. 271 (1996) 20353–20358.

[169] R. Benoit, D. Frey, M. Hilbert, J. Kevenaar, M. Wieser, C. Stirnimann, et al., Structural basis for recognition of synaptic vesicle protein 2C by botulinum neurotoxin A., Nature. 505 (2014) 108–11.

[170] J. Wagman, J. Bateman, Botulinum Type A Toxin: Properties of a Toxic Dissociation Product, Arch. Biochem. Biophys. 45 (1952) 375–383.

[171] J. Wagman, J. Bateman, The behavior of the botulinus toxin in the ultracentrifuge, Arch. Biochem. Biophys. 31 (1951) 424–430.

[172] J. Wagman, Low molecular weight forms of type A botulinum toxin. II. Action of pepsin on intact and dissociated toxin, Arch. Biochem. Biophys. 100 (1963) 414–421.

[173] K.-H. Eisele, K. Fink, M. Vey, H. Taylor, Studies on the dissociation of botulinum neurotoxin type A complexes., Toxicon. 57 (2011) 555–65.

110

[174] G. Tortora, B. Derrickson, Principles of Anatomy and Physiology, 12th ed., Hoboken, 2009.

[175] S. Rune, K. Viskum, Duodenal pH values in normal controls and in patients with duodenal ulcer., Gut. 10 (1969) 569–71.

[176] A. Maksymowych, L. Simpson, Binding and transcytosis of botulinum neurotoxin by polarized human colon carcinoma cells., J. Biol. Chem. 273 (1998) 21950–7.

[177] A. Couesnon, Y. Pereira, M. Popoff, Receptor-mediated transcytosis of botulinum neurotoxin A through intestinal cell monolayers., Cell. Microbiol. 10 (2008) 375–87.

[178] D. Ancharski, A. Singh, Z. Nasser, R. Olson, L. Simpson, Evidence That Botulinum Toxin Receptors on Epithelial Cells and Neuronal Cells Are Not Identical: Implications for Development of a Non-Neurotropic Vaccine, J. Pharmacol. Exp. Ther. 336 (2011) 605–612.

[179] Y. Fujinaga, Interaction of botulinum toxin with the epithelial barrier., J. Biomed. Biotechnol. 2010 (2010) 974943.

[180] S. Sugii, I. Ohishi, G. Sakaguchi, Correlation between oral toxicity and in vitro stability of Clostridium botulinum type A and B toxins of different molecular sizes., Infect. Immun. 16 (1977) 910–4.

[181] S. Sugii, I. Ohishi, G. Sakaguchi, Intestinal absorption of botulinum toxins of different molecular sizes in rats., Infect. Immun. 17 (1977) 491–6.

[182] A. Maksymowych, M. Reinhard, C.J. Malizio, M.C. Goodnough, E. a Johnson, L.L. Simpson, Pure botulinum neurotoxin is absorbed from the stomach and small intestine and produces peripheral neuromuscular blockade., Infect. Immun. 67 (1999) 4708–12.

[183] K. Lee, S. Gu, L. Jin, T.T.N. Le, L.W. Cheng, J. Strotmeier, et al., Structure of a bimodular botulinum neurotoxin complex provides insights into its oral toxicity., PLoS Pathog. 9 (2013) e1003690.

[184] K. Lee, K.-H. Lam, A.M. Kruel, K. Perry, A. Rummel, R. Jin, High-resolution crystal structure of HA33 of botulinum neurotoxin type B progenitor toxin complex., Biochem. Biophys. Res. Commun. 446 (2014) 568–573.

[185] T. Nakamura, T. Tonozuka, A. Ide, T. Yuzawa, K. Oguma, A. Nishikawa, Sugar-binding sites of the HA1 subcomponent of Clostridium botulinum type C progenitor toxin., J. Mol. Biol. 376 (2008) 854–67.

[186] S. Yamashita, H. Yoshida, N. Uchiyama, Y. Nakakita, S. Nakakita, Carbohydrate recognition mechanism of HA70 from Clostridium botulinum deduced from X-ray structures in complexes with sialylated oligosaccharides, FEBS Lett. 586 (2012) 2404–2410.

[187] S. Arnon, Human Teatanus and Human Botulism, in: J. Rood, B. McClane, J. Songer, R. Titball (Eds.), Clostridia Mol. Biol. Pathog., Academic Press, Inc., San Diego, 1997: pp. 95–115.

[188] L. Simpson, Identification of the major steps in botulinum toxin action., Annu. Rev. Pharmacol. Toxicol. 44 (2004) 167–93.

[189] I. Ohishi, G. Sakaguchi, Oral toxicities of Clostridium botulinum type Oral Toxicities of Clostridium botulinum Type C and D Toxins of Different Molecular Sizes, Infect. Immun. 28 (1980) 303–309.

[190] Y. Fujinaga, K. Inoue, S. Watanabe, K. Yokota, Y. Hirai, E. Nagamachi, et al., The haemagglutinin of of Clostridium botulinum type C progenitor toxin plays an essential role in binding of toxin to the epithelial cells of guinea pig small intestine, leading to the efficient absorption of the toxin, Microbiology. 143 (1997) 3841–3847.

[191] N. Uotsu, A. Nishikawa, T. Watanabe, T. Ohyama, T. Tonozuka, Y. Sakano, et al., Cell internalization and traffic pathway of Clostridium botulinum type C neurotoxin in HT-29 cells., Biochim. Biophys. Acta. 1763 (2006) 120–8.

[192] Y. Fujinaga, K. Inoue, T. Nomura, J. Sasaki, J. Marvaud, M.R. Popo, et al., Identification and characterization of functional subunits of Clostridium botulinum type A progenitor toxin involved in binding to intestinal microvilli and erythrocytes, FEBS Lett. 467 (2000) 179–183.

[193] T. Matsumura, Y. Jin, Y. Kabumoto, Y. Takegahara, K. Oguma, W.I. Lencer, et al., The HA proteins of botulinum toxin disrupt intestinal epithelial intercellular junctions to increase toxin absorption., Cell. Microbiol. 10 (2008) 355–64.

[194] F. Burkard, F. Chen, G. Kuziemko, R. Stevens, Electron density projection map of the botulinum neurotoxin 900-kilodalton complex by electron crystallography., J. Struct. Biol. 120 (1997) 78–84.

[195] K. Hasegawa, T. Watanabe, T. Suzuki, A. Yamano, T. Oikawa, Y. Sato, et al., A novel subunit structure of Clostridium botulinum serotype D toxin complex with three extended arms., J. Biol. Chem. 282 (2007) 24777–83.

[196] M. Radermacher, T. Wagenknecht, A. Vershoor, J. Frank, Three-dimensional reconstruction from a single-exposure, randome conical tilt series applied to the 50S ribosomal subunit of Escherichia coli, J. Micoscopy. 146 (1987) 113–136.

[197] M. Ohi, Y. Li, Y. Cheng, T. Walz, Negative Staining and Image Classification - Powerful Tools in Modern Electron Microscopy., Biol. Proced. Online. 6 (2004) 23–34.

[198] J. Frank, M. Radermacher, P. Penczek, J. Zhu, Y. Li, M. Ladjadj, et al., SPIDER and WEB: processing and visualization of images in 3D electron microscopy and related fields., J. Struct. Biol. 116 (1996) 190–9.

[199] E.F. Pettersen, T. Goddard, C.C. Huang, G.S. Couch, D.M. Greenblatt, E.C. Meng, et al., UCSF Chimera--a visualization system for exploratory research and analysis., J. Comput. Chem. 25 (2004) 1605–12.

[200] S. Adekar, T. Takahashi, R.M. Jones, F. Al-Saleem, D. Ancharski, M.J. Root, et al., Neutralization of botulinum neurotoxin by a human monoclonal antibody specific for the catalytic light chain., PLoS One. 3 (2008) e3023.

[201] M. Kitamura, S. Sakaguchi, G. Sakaguchi, Significance of 12S toxin of Clostridium botulinum type E., J. Bacteriol. 98 (1969) 1173–8.

[202] S. Miyazaki, S. Kozaki, S. Sakaguchi, G. Sakaguchi, Comparison of progenitor toxins of nonproteolytic with those of proteolytic Clostridium botulinum Type B., Infect. Immun. 13 (1976) 987–9.

[203] J. Wagman, Isolation and sedimentation study of low molecular weight forms of type A Botulins toxin, Arch. Biochem. Biophys. 50 (1954) 104–112.

[204] T. Nakamura, T. Tonozuka, S. Ito, Y. Takeda, R. Sato, I. Matsuo, et al., Molecular diversity of the two sugar-binding sites of the beta-trefoil lectin HA33/C (HA1) from Clostridium botulinum type C neurotoxin, Arch. Biochem. Biophys. 512 (2011) 69–77.

[205] K. Inoue, Structural analysis by X-ray crystallography and calorimetry of a haemagglutinin component (HA1) of the progenitor toxin from Clostridium botulinum, Microbiology. 149 (2003) 3361–3370.

[206] T. Nishiki, Y. Tokuyama, Y. Kamata, Y. Nemoto, a Yoshida, K. Sato, et al., The high-affinity binding of Clostridium botulinum type B neurotoxin to synaptotagmin II associated with gangliosides GT1b/GD1a., FEBS Lett. 378 (1996) 253–7.

[207] M. Popoff, Ecology of neurotoxigenic strains of Clostridia, Curr. Top. Microbiol. Immunol. 195 (1995) 1–29.

[208] G. Bergey, W. Habig, J. Bennett, C. Lin, Proteolytic cleavage of tetanus toxin increases activity., J. Neurochem. 53 (1989) 155–61.

[209] C. Chen, Z. Fu, J.-J. Kim, J. Barbieri, M. Baldwin, Gangliosides as high affinity receptors for tetanus neurotoxin., J. Biol. Chem. 284 (2009) 26569–77.

[210] S. Rinaldi, K. Brennan, C. Goodyear, C. O'Leary, G. Schiavo, P. Crocker, et al., Analysis of lectin binding to glycolipid complexes using combinatorial glycoarrays., Glycobiology. 19 (2009) 789–96.

[211] F. Blum, C. Chen, A. Kroken, J. Barbieri, Tetanus toxin and botulinum toxin a utilize unique mechanisms to enter neurons of the central nervous system., Infect. Immun. 80 (2012) 1662–9.

[212] J. Farrar, L. Yen, T. Cook, N. Fairweather, N. Binh, J. Parry, et al., Tetanus, J Neurol Neurosurg Psychiatry. 69 (2000) 292–301.

[213] L. Pillemer, R. Wittler, D. Grossberg, The Isolation and Crystallization of Tetanal Toxin, Science, 103 (1946) 615–616.

[214] H. Sato, A. Ito, Y. Yamakawa, R. Murata, Toxin-Neutralizing Effect of Antibody Against Subtilisin-Digested Tetanus Toxin, Indian J. Med. Res. 24 (1979) 958–961.

[215] W. Chiu, D. Rankert, M. Cumming, J. Robinson, Characterization of crystalline filtrate tetanus toxin, J. Ultrastruct. Res. 79 (1982) 285–293.

[216] J. Robinsons, L. Holladay, J. Hash, D. Puett, Conformational and Molecular Weight Studies of Tetanus Toxin and Its Major Peptides, J. Biol. Chem. 257 (1982) 407–411.

[217] B. Singh, M. Fuller, G. Schiavo, Molecular structure of tetanus neurotoxin as revealed by Fourier transform infrared and circular dichroic spectroscopy., Biophys. Chem. 36 (1990) 155–66.

[218] J. Robinson, M. Schmid, D. Morgan, W. Chiu, Three-dimensional structural analysis of tetanus toxin by electron crystallography., J. Mol. Biol. 200 (1988) 367–75.

[219] S.J. Ludtke, P.R. Baldwin, W. Chiu, EMAN: semiautomated software for high-resolution single-particle reconstructions., J. Struct. Biol. 128 (1999) 82–97.

[220] T.R. Shaikh, H. Gao, W. Baxter, F. Asturias, N. Boisset, A. Leith, et al., SPIDER image processing for single-particle reconstruction of biological macromolecules from electron micrographs., Nat. Protoc. 3 (2008) 1941–74.

[221] M. Hohn, G. Tang, G. Goodyear, P.R. Baldwin, Z. Huang, P. a Penczek, et al., SPARX, a new environment for Cryo-EM image processing., J. Struct. Biol. 157 (2007) 47–55.

[222] G. Tang, L. Peng, P. Baldwin, D. Mann, W. Jiang, I. Rees, et al., EMAN2: an extensible image processing suite for electron microscopy., J. Struct. Biol. 157 (2007) 38–46.

[223] A. Fischer, C. Garcia-Rodriguez, I. Geren, J. Lou, J. Marks, T. Nakagawa, et al., Molecular architecture of botulinum neurotoxin E revealed by single particle electron microscopy., J. Biol. Chem. 283 (2008) 3997–4003.

[224] R. Agarwal, S. Eswaramoorthy, D. Kumaran, T. Binz, S. Swaminathan, Structural analysis of botulinum neurotoxin type E catalytic domain and its mutant Glu212-->Gln reveals the pivotal role of the Glu212 carboxylate in the catalytic pathway., Biochemistry. 43 (2004) 6637–44.

[225] S. Gu, S. Rumpel, J. Zhou, J. Strotmeier, Botulinum neurotoxin is shielded by NTNHA in an interlocked complex, Science (80-.). 335 (2012) 977–981.

[226] Y. Sagane, T. Watanabe, H. Kouguchi, H. Sunagawa, S. Obata, K. Oguma, et al., Spontaneous nicking in the nontoxic-nonhemagglutinin component of the Clostridium botulinum toxin complex, Biochem. Biophys. Res. Commun. 292 (2002) 434–440.

[227] K. Krebs, F. Lebeda, Comparison of the structural features of botulinum neurotoxin and NTNH, a non-toxic accessory protein of the progenitor complex, Botulinum J. 1 (2008) 116–134.

[228] K. Miyata, T. Yoneyama, T. Suzuki, H. Kouguchi, K. Inui, K. Niwa, et al., Expression and stability of the nontoxic component of the botulinum toxin complex., Biochem. Biophys. Res. Commun. 384 (2009) 126–130.

[229] R. Fujita, Y. Fujinaga, K. Inoue, H. Nakajima, H. Kumon, K. Oguma, Molecular characterization of two forms of nontoxic-nonhemagglutinin

components of Clostridium botulinum type A progenitor toxins., FEBS Lett. 376 (1995) 41–4.

[230] C.L. Wellst, E. Balish, Clostridium tetani growth and toxin production in the intestines of germfree rats, Infect. Immun. 41 (1983) 826–828.

[231] C. Cooksley, I. Davis, K. Winzer, W. Chan, M. Peck, N. Minton, Regulation of neurotoxin production and sporulation by a Putative agrBD signaling system in proteolytic Clostridium botulinum., Appl. Environ. Microbiol. 76 (2010) 4448–60.